Journal of
Medicinal Chemistry

Article

Intracellular Trapping of the Selective Phosphoglycerate Dehydrogenase (PHGDH) Inhibitor BI-4924 Disrupts Serine Biosynthesis

Harald Weinstabl, Matthias Treu, Jörg Rinnenthal, Stephan Zahn, Peter Ettmayer, Gerd Bader, Georg Dahmann, Dirk Kessler, Klaus Rumpel, Nikolai Mischerikow, Fabio Savarese, Thomas Gerstberger, Moriz Mayer, Andreas Zoephel, Renate Schnitzer, Wolfgang Sommergruber, Paola Martinelli, Heribert Arnhof, Biljana Peric Simov, Karin Stephanie Hofbauer, Géraldine Garavel, Yvonne Scherbantin, Sophie Mitzner, Thomas Fett, Guido Scholz, Jens Bruchhaus, Michelle Burkard, Roland Kousek, Tuncay Ciftci, Bernadette Sharps, Andreas Schrenk, Christoph Harrer, Daniela Haering, Bernhard Wolkerstorfer, Xuechun Zhang, Xiaobing Lv, Alicia Du, Dongyang Li, Yali Li, Jens Quant, Mark Pearson, and Darryl B. McConnell

J. Med. Chem., **Just Accepted Manuscript** • Publication Date (Web): 31 Jul 2019

Just Accepted

is published by the American Chemical Society. 1155 Sixteenth Street N.W., Washington, DC 20036

	Lv, Xiaobing; ChemPartner Du, Alicia; ChemPartner Li, Dongyang; ChemPartner Li, Yali; ChemPartner Quant, Jens; Boehringer Ingelheim RCV GmbH & Co KG Pearson, Mark; Boehringer Ingelheim RCV GmbH und Co KG McConnell, Darryl; Boehringer Ingelheim RCV GmbH und Co KG

Intracellular Trapping of the Selective Phosphoglycerate Dehydrogenase (PHGDH) Inhibitor BI-4924 Disrupts Serine Biosynthesis

Harald Weinstabl[†, §,‡], Matthias Treu[§, ‡], Joerg Rinnenthal[§], Stephan K. Zahn[§], Peter Ettmayer[§], Gerd Bader[§], Georg Dahmann[§], Dirk Kessler[§], Klaus Rumpel[§], Nikolai Mischerikow[§], Fabio Savarese[§], Thomas Gerstberger[§], Moriz Mayer[§], Andreas Zoephel[§], Renate Schnitzer[§], Wolfgang Sommergruber[§], Paola Martinelli[§],Heribert Arnhof[§], Biljana Peric-Simov[§], Karin S. Hofbauer[§], Géraldine Garavel[§], Yvonne Scherbantin[§], Sophie Mitzner[§], Thomas N. Fett[§], Guido Scholz[§], Jens Bruchhaus[§], Michelle Burkard[§], Roland Kousek[§], Tuncay Ciftci[§], Bernadette Sharps[§], Andreas Schrenk[§], Christoph Harrer[§], Daniela Haering[§], Bernhard Wolkerstorfer[§], Xuechun Zhang[#], Xiaobing Lv[#], Alicia Du[#], Dongyang Li[#], Yali Li[#], Jens Quant[§], Mark Pearson[§], Darryl B. McConnell[§]

[§]Boehringer Ingelheim RCV GmbH & Co KG; Dr.-Boehringer-Gasse 5-11, 1121 Vienna, Austria

[$]Boehringer Ingelheim Pharma GmbH & Co. KG; Birkendorfer Str. 65, 88400 Biberach an der Riß, Germany

[#]Shanghai ChemPartner Co., LTD., No. 5 Building, 998 Halei Road, Zhangjiang Hi-Tech Park Pudong New Area, Shanghai China, 201203

PHGDH, inhibitor, NAD^+ competitive, (tumor) metabolism, cancer, *in vitro* PK-PD

ABSTRACT

Phosphoglycerate dehydrogenase (PHGDH) is known to be the rate limiting enzyme in the serine synthesis pathway (SSP) in humans. It converts glycolysis derived 3-phosphoglycerate to 3-phosphopyruvate in a NADH/NAD^+-dependent oxidation

reaction. Herein we report the discovery of **BI-4916**, a prodrug of the NADH/NAD^+-competitive PHGDH inhibitor **BI-4924** which has shown high selectivity against the majority of other dehydrogenase targets. Starting with a fragment-based screening (FBS) a subsequent hit optimization using structure based drug design (SBDD) was conducted to deliver a single digit nanomolar lead series and to improve potency by six orders of magnitude. To this end, an intracellular ester cleavage mechanism of the ester prodrug was utilized to achieve intracellular enrichment of the actual carboxylic acid based drug and thus overcome high cytosolic levels of the competitive cofactors NADH/NAD^+.

INTRODUCTION

Cancer cells can rewire their metabolism to support fast growth and proliferation, and indeed the “deregulation of cellular energetics” has been included among the hallmarks of cancer.[1] Metabolic enzymes have therefore raised interest as potential targets for therapies aimed at “fasting” cancer cells.

Phosphoglycerate dehydrogenase (PHGDH), an enzyme in the serine synthesis pathway,[2] has been found to be involved in numerous cancers such as breast cancer,[3, 4] melanoma,[5] pancreatic cancer,[6] kidney cancer,[7, 8] and non-small cell lung cancer,[9] as well as in pulmonary fibrosis.[10] *PHGDH*, the gene coding for phosphoglycerate dehydrogenase, was found to be focally amplified or gained in melanoma and breast cancer,[3, 4] where it is broadly overexpressed in about 70% of triple-negative cases even in the absence of amplification. Cells with *PHGDH* amplification and overexpression were shown to be highly sensitive to its depletion. A subgroup of PHGDH-overexpressing tumors was also observed among non-small cell lung cancer and lung adenocarcinoma cases and also in this case PHGDH knock-down selectively impaired the growth of overexpressing cells, suggesting an oncogenic function of PHGDH.[9, 11]

In more detail, a negative-selection RNAi screening using an orthotopic human breast cancer xenograft model was developed by Possemato *et al*. in 2011 identifying PHGDH as a gene required for *in vivo* tumorigenesis.[3] in addition, PHGDH was shown to be localized in a genomic region of recurrent copy number gain in breast cancer

particularly in ER-negative or triple negative breast cancers.[12] Similarly, PHGDH is recurrently amplified in a genomic region of focal copy number gain most commonly found in melanoma. Knockdown of PHGDH selectively inhibited the growth of melanoma cells that exhibit PHGDH amplification versus those that lack this amplification.[4, 5] PHGDH protein expression was recently correlated with advanced TNM stage, larger tumor size and poor outcomes in colorectal cancer patients.[13] Studies utilizing a large panel of NSCLC cell lines revealed that NRF2 controls the expression of the PHGDH gene and that PHGDH confers poor prognosis in human NSCLC.[9] Recently, a strong antiproliferative effect was shown in a pancreatic xenograft model by inhibition of PHGDH with IoxA, a natural withanolide.[14]

PHGDH is the rate limiting enzyme in the serine synthesis pathway in humans which diverts 3-phosphoglycerate from glycolytic serine biosynthesis by oxidizing it to 3-phosphopyruvate in a NADH/NAD^+-dependent manner (Figure 1).[2] Subsequently, 3-phosphopyruvate is converted to serine by phosphoserine transaminase and phosphoserine hydrolase. Serine is regarded as a non-essential amino acid, however, it

is indispensable and plays a critical role in several cellular processes such as the conversion to glycine supporting the backbone of central carbon metabolism (carbon unit for purine synthesis),[15] the generation of sphingosine via reaction with palmitoyl-CoA,[16] the regulation of redox potential (production of NADPH)[17] and as a precursor of other amino acids (e.g. cysteine)[16]. It is apparent that cells with PHGDH amplification and/or high expression are not sensitive to serine depletion, indicating the loss of proliferation upon knockdown of PHGDH is not simply due to reduction in serine levels *per se*.[3] Although a plethora of published data supports the contribution of the serine synthesis pathway to tumorigenesis, in particular the role of the key enzyme PHGDH, only recently the precise molecular mechanism of PHGDH in oncogenesis has been characterized in detail. Inhibition of PHGDH alters nucleotide metabolism in a way that is independent of serine utilization and redox maintenance. Mechanistically, it rather results in disruption of mass balance within central carbon metabolism leading to alterations in both the pentose phosphate pathway (PPP) and the tri-carboxylic acid cycle (TCA).[18] Indeed, restoration of the TCA cycle and PPP through addition of ribose and cell-permeable α-ketoglutarate to PHGDH-inhibitor treated tumor cells was

sufficient to rescue the antiproliferative effect generated by PHGDH inhibition. In their study, Reid and colleagues clearly showed that the mass balance and the requirement of maintaining flux balance is sufficient to regulate the flux into other neighboring anabolic pathways such as glycolysis and the TCA cycle.[18]

The lack of serine derived glutathione (GSH) has been reported to underlie the increased sensitivity towards reactive oxygen species (ROS) of tumor cells lacking PHGDH.[19] PHGDH has been further demonstrated to be able to use α-ketoglutarate as a substrate to produce the oncometabolite D-2-hydroxyglutarate (D-2-HG), perhaps linking PHGDH activity with changes in the epigenetic program of amplified tumor cells.[20] However, as the PHGDH enzymatic activity towards 2-hydroxyglutarate production is extremely low compared to 3-phosphohydroxypyruvate it remains to be determined if those levels of 2-hydroxyglutarate produced by PHGDH do play a similar role in the epigenetic re-programming as it was shown for the mutated isocitrate-dehydrogenase 1 and 2 in glioma and AML.[21, 22] (Figure 1)

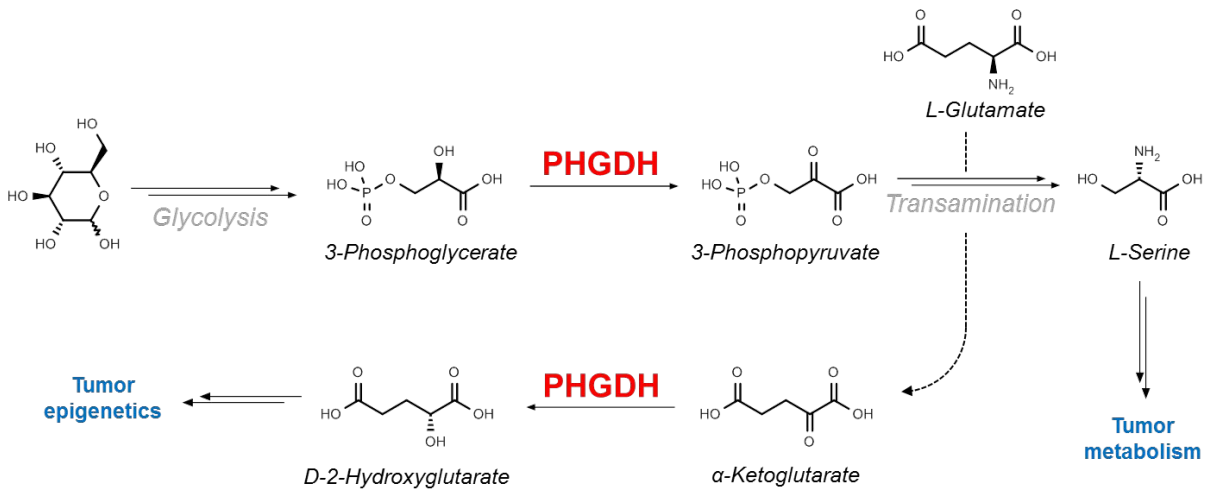

Figure 1: Known roles of PHGDH in tumor metabolism and tumor epigenetics

In preclinical models, breast and pancreatic adenocarcinomas have been shown to be dependent on the SSP suggesting that PHGDH may represent a therapeutic intervention point.[2] Developing highly potent and specific PHGDH inhibitors will promote understanding of the molecular mechanisms triggering the dependency of certain tumor (sub)types on this pathway but also opens a novel therapeutic opportunity to treat those tumors. This emphasizes the need for compounds exhibiting low nanomolar cellular potency and exquisite specificity to enable better understanding of the target in a cellular context.

The challenge when targeting metabolic enzymes in a competitive fashion is intrinsically tied to competing with millimolar intracellular levels of the cofactor NAD^+ and NADH accompanied by the fact that modulation of metabolic targets often need high levels of target occupancy to achieve efficacy.[23] Preceding in house target validation experiments and data published by Chen *et. al*. strengthen this hypothesis. The authors showed that > 90% PHGDH knockdown over 14 days was anti-proliferative in PHGDH high breast cancer cell lines and in line with this observation < 90% knockdown *in vivo* was not associated with tumor growth inhibition – indeed defining the level and duration of inhibition of a given target required for efficacy is essential in order to design appropriate drugs.[24] Furthermore, PHGDH exhibits a polar shallow cofactor/substrate binding pocket which makes the druggability of PHGDH extremely challenging.

Several compounds are reported in literature to inhibit PHGDH which can be divided in two groups: allosteric inhibitors, such as CBR-5884 (**2**),[25] NCT-503 (**3**),[26] "compound 34" (**5**) and PKUMDL-WQ-2201 (**7**) display a micromolar potency and are not dependent on intracellular cofactor levels.[27, 28] On the other hand, orthosteric inhibitors,

such as Astra Zeneca's indole-2-carboxamide **1** and fragment **6** are validated adenosine pocket binders thus underlying the competitive binding of the natural cofactor NADH/ NAD^+.[29, 30] Compound **4** discovered by RAZE pharmaceuticals is likely to share the same binding mode due to structural similarity.[31]

Herein we report on the discovery of a prodrug-based NADH/NAD^+-competitive PHGDH inhibitor with high selectivity (based on proteomics ANOVA analysis) against the majority of other dehydrogenase targets. An intracellular ester cleavage mechanism of the permeable ester prodrug **BI-4916** was utilized to achieve intracellular enrichment of the actual carboxylic acid based poorly permeable drug **BI-4924** and thus to overcome high intracellular levels of the competitive cofactor NADH/NAD^+. Compound **1** and **BI-4924** are X-ray validated NAD^+ competitive binders. Compounds **3** (NCT-503; thiourea) and **5** ("compound 34"; thioamide) and **7** (thiosemicarbazide) exhibit potentially reactive PAINS motives.[25-33]

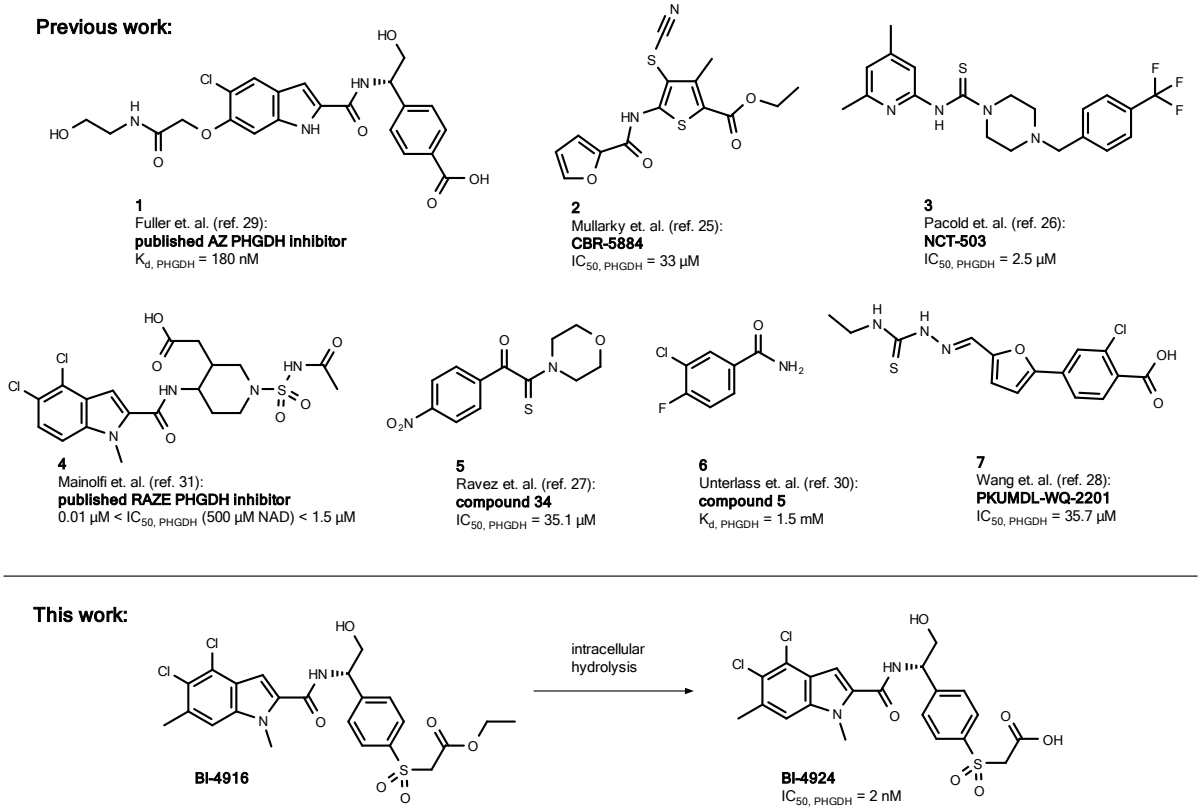

Figure 2: Overview of selected published PHGDH inhibitors and reported binding/inhibition data.

RESULTS AND DISCUSSION

Screening:

Screening was performed in two different hit finding approaches (Figure 3). First, a high throughput screen (HTS) was performed based on a pool consisting of > 1,000,000 molecular entities. Within this approach, no boundaries were set and allosteric as well as orthosteric binders were evaluated with a biochemical NAD^+-dependent screening cascade. Second, a fragment based screen (FBS) was conducted in parallel.

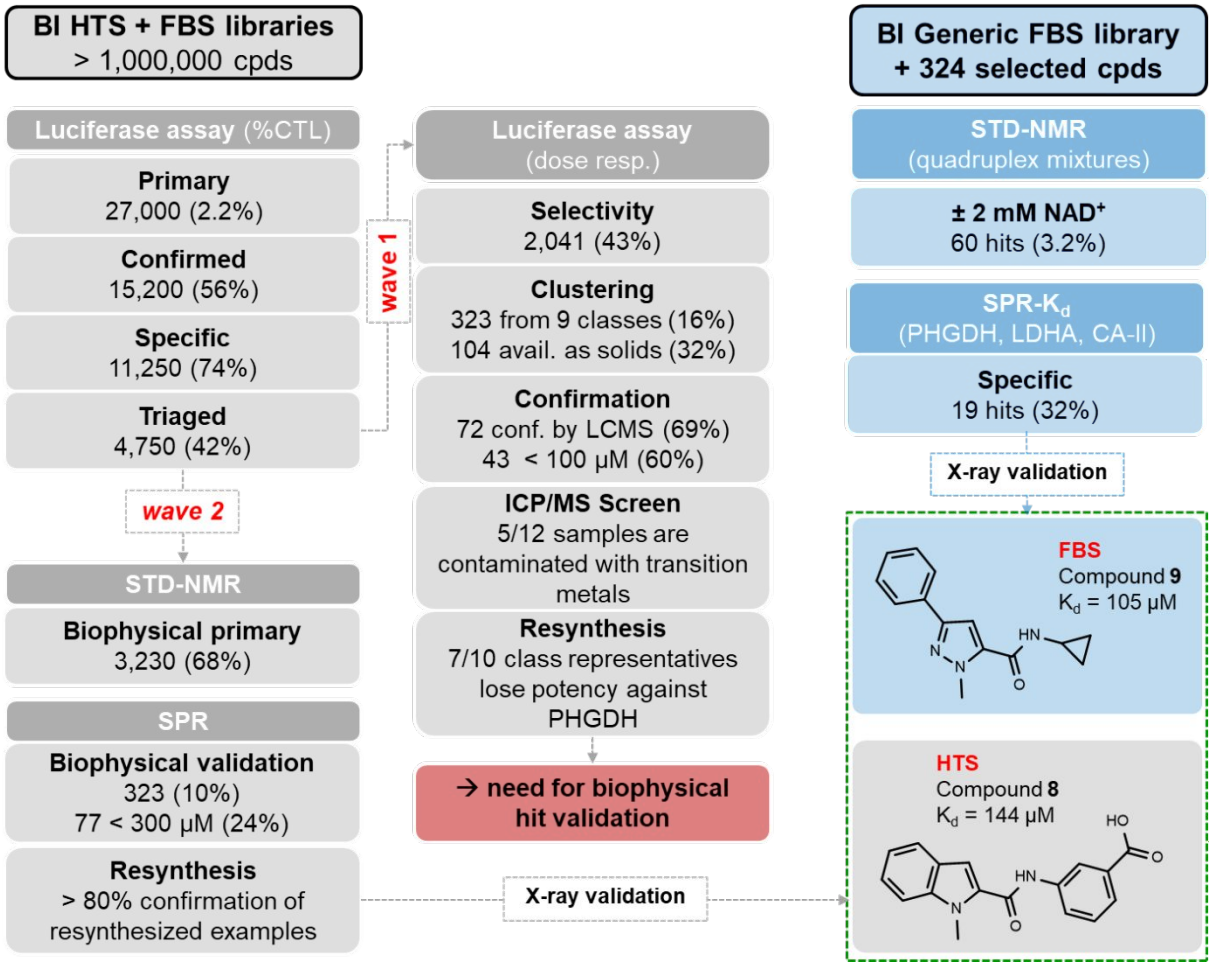

Figure 3: Schematic representation of the hit finding process. Saturation Transfer Difference NMR (STD-NMR) guided based FBS screening on the right (blue) and luciferase based HTS screening on the left (grey).

High Throughput Screen (HTS): HTS yielded 27,000 primary hits (2.2% hit rate). The confirmed hits (15,200; 56% of primary hits) were profiled in a shortcut assay containing

no PHGDH, and dual hitters were removed as false positives (11,250 compounds remaining; 74% of confirmed hits). These hits were triaged to 4,750 (42%) hits by removal of unwanted substructures (e.g. PAINS)[33] and compounds with MW ≥ 600 and clogP ≥ 5.5. For these triaged hits, dose response curves were measured in PHGDH, lactate dehydrogenase (subtype A; LDHA) and shortcut assays. Thus, 2,041 potent and selective PHGDH inhibitors were progressed to cluster analysis. 323 representative hits from 9 classes and singletons of interest were prioritized. The purity of 72 out of 104 class representatives was confirmed by LC/MS using freshly prepared DMSO stock solutions. 43 out of these 72 were confirmed as selective PHGDH inhibitors (> 10-fold selectivity towards LDHA) with an IC_{50} < 100 μM. Due to the fact that many of these hits (triazoles, aryl-pyrazoles) have been synthesized employing transition metal catalysis and that dehydrogenases often show a high sensitivity towards transition metals,[34] a selection of metal ions was tested in the biochemical assays. It was discovered that transition metal ions (e.g. Hg, Cu, Pt, Pd) are potent inhibitors of PHGDH and indeed, for 5 out of 12 selected HTS hits Hg and Cu impurities were quantified (68 elements screened by ICP-MS) in sufficient concentrations to explain the observed PHGDH

inhibition. In line with this finding, it was not surprising that 7 out of 10 resynthesized and purified HTS hits lost their PHGDH inhibition.

As a consequence, STD-NMR with and without NAD^+ and SPR were applied for orthogonal hit validation. The latter was found to tolerate metal impurities (only Pd^{2+} shows a measureable K_d of significance) and the paramagnetic nature of copper leads to line broadening in STD-NMR.[35] As a next step, we went back to the 4,750 confirmed actives and performed a cluster analysis to selected 3,230 (68%) hits for re-screening at 50 µM for specific binding to PHGDH in the SPR assay. From the identified 323 (10%) PHGDH binders, 77 had a K_d < 300 µM which were again clustered according to their chemical structure. This orthogonal HTS hit validation strategy translated in >80 % SPR K_d confirmation for the re-synthesized cluster representatives and resulted in three chemical series with X-ray derived binding mode information among which compound **8** (indole-2-carboxamide) is a representative example.

Fragment based screening (FBS): A truncated version of human PHGDH according to a previously published structure (PDB code: 2G76,

https://www.thesgc.org/structures/2g76) was designed (A4-V315; see supporting information), expressed and purified in gram quantities. In contrast to the full length protein (tetramer), it was found to be active as a dimer in solution and was also used for the biochemical assay as well as crystallographic analysis. FBS aimed at finding NAD-orthosteric binders, thus a NAD stripping protocol was developed for the preparation of PHGDH apo-protein. An in-house library of 1,536 fragments was complemented by a customized library of 324 soluble (> 100 µM aqueous solubility) based on fragments selected based on learnings from a LDHA fragment based screening campaign.[34]

A total of 1,860 fragments were screened in quadruplex mixtures by STD-NMR (250 µM fragment and 20 µM apo-protein) to reduce the time requirements of the screening campaign. STD-NMR spectra for the individual hits from 10 mixtures with > 40% STD signal and 59 mixtures with > 20% STD signal were recorded with and without NAD (2 mM). 60 hits (3.2% hit rate) were identified that bind preferentially to the apo-protein and in a less pronounced manner to the NAD bound protein. SPR-K_d-values for PHGDH,

lactate dehydrogenase, and carbonic anhydrase II were measured for these 60 compounds, resulting in the identification of 19 specific PHGDH binders (32% hit rate).

The development of a low temperature co-crystallization protocol allowed the X-ray-validation of an adenine pocket binder **9** out of the phenylpyrazole-5-carboxamide series (2.15 Å resolution). This fragment shows a strong interaction with D174 and thus exhibits suitable vectors along the NAD^+-binding site (Figure 4).

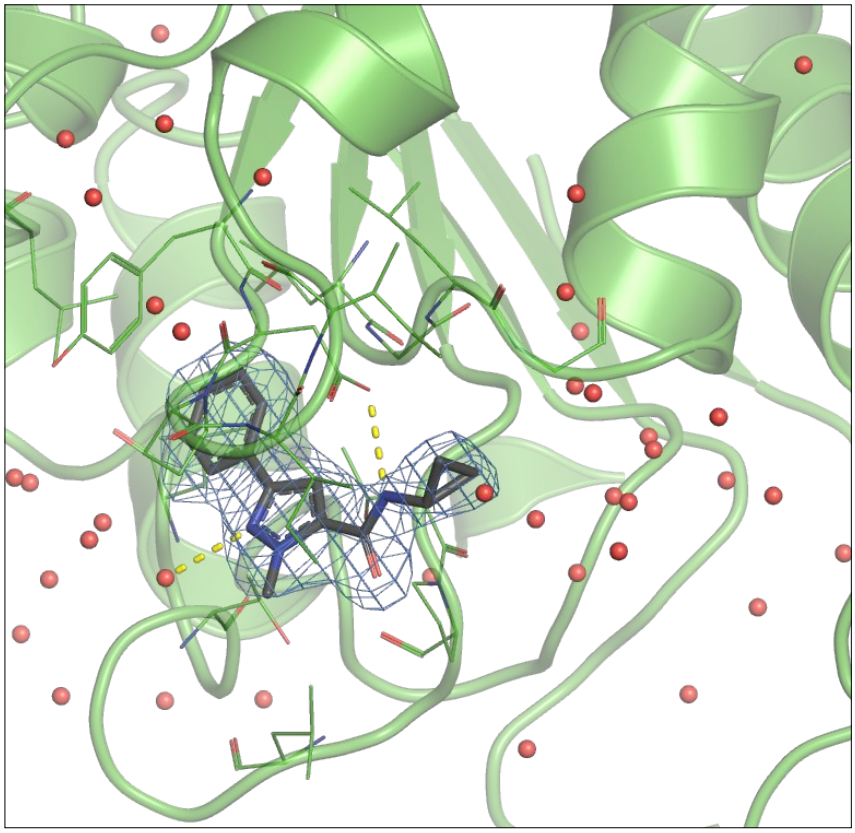

Figure 4: Validated hit from the STD-NMR FBS screen: phenylpyrazole-5-carboxamide **9** co-crystallized with PHGDH showing the main polar interaction to D174 (PDB code: **6RIH**).

All hits identified bind orthosterically to the lipophilic adenine pocket and form a H-bond to D174.

Structural Analysis of PHGDH in Complex with its natural Cofactor and Substrate

Co-crystallization of PHGDH with its natural substrate 3-PG was performed to gain more insight into the catalytic mechanism of the enzyme and to enable the structure based design of transition state analogues. The binding mode of the cofactor NAD^+ was found to be identical to previously published structures of human PHGDH (Figure 5). The sequence of murine PHGDH shows a high degree of similarity (98.5%) as well as identity (94.6%). Briefly, the nicotinamide (NA) interacts with the backbone of C233 and A285 and the sidechain of D259. The ribose of the nicotinamide part as well as the

linking phosphates form numerous direct and water mediated hydrogen bonds with the protein. The main directed interaction of the adenosine moiety is the hydrogen bonding of the ribose hydroxyl groups with the side chain of D174. In a recent publication, L-tartrate, derived from the crystallization buffer, bound in one of the two active sites and was discussed as an analogue of the natural substrate.[36] In our structure (PDB code: 6CWA), 3-PG indeed binds to the same positon as the L-tartrate. The phosphate group forms extensive interactions with the side chains of R53, S54 and R74 of monomer A as well as R134 of monomer B. Also, the rest of the 3-PG moiety is part of an extensive hydrogen bonding network with the active site of PHGDH.

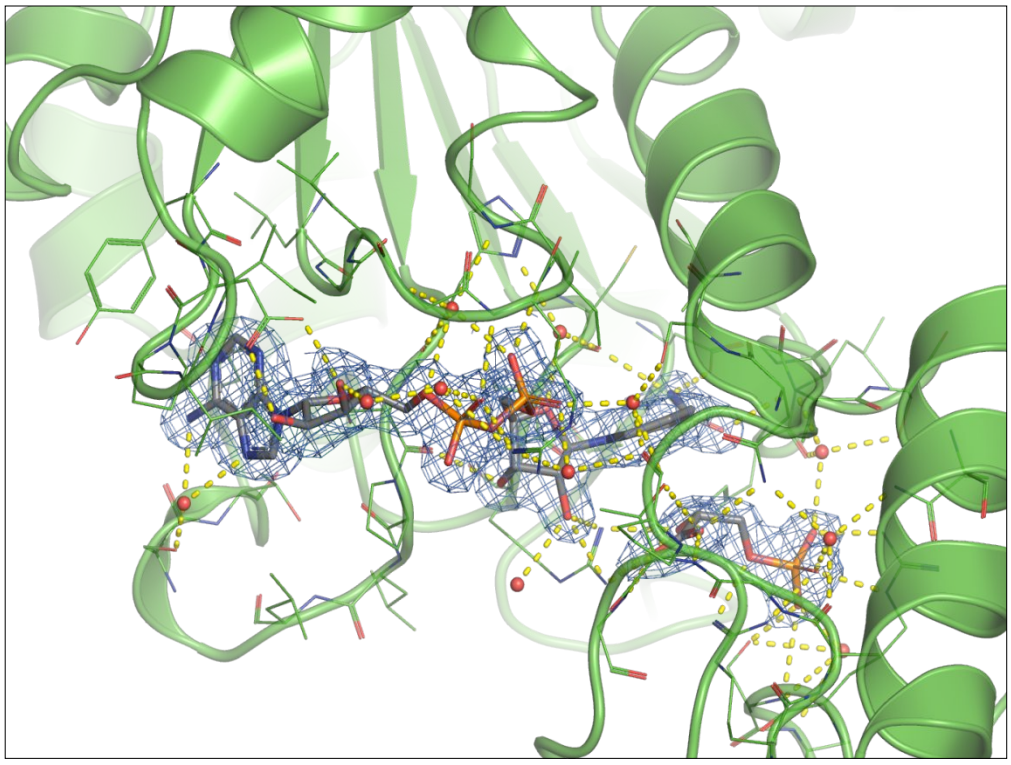

Figure 5: Electron density map of ternary complex of cofactor NAD^+ and substrate 3-PG in PHGDH (PDB code: 6CWA)

Structure Based Compound Optimization

Scheme 1: General Overview of the hit optimization

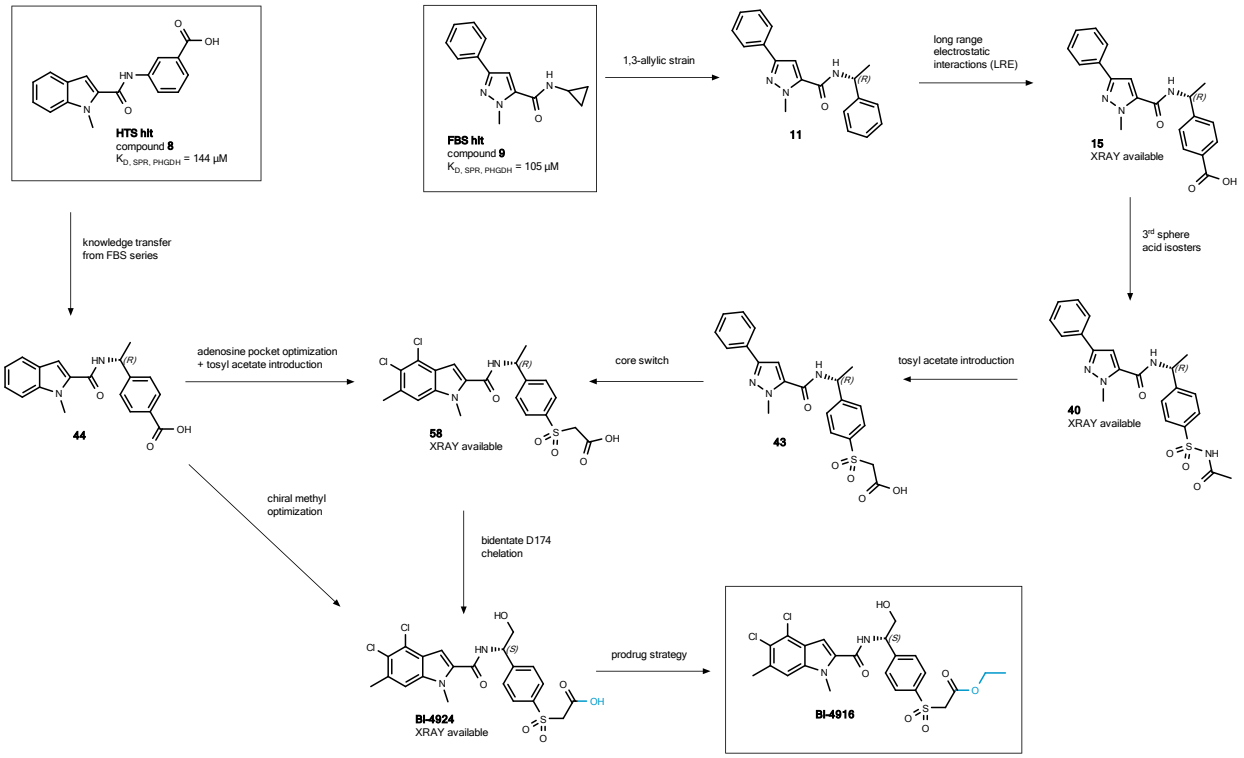

Double tracked strategy: Merging learnings from HTS and FBS leads to **BI-4924** and **BI-4916**

Both hit classes – (phenylpyrazole-5-carboxamides from the FBS and indole-2-carboxamides from the HTS (Scheme 1) – form a H-bond to the side-chain of D174 and the amide NH of the ligand. This acts as a polar anchor to place a lipophilic aromatic motif in the corresponding hydrophobic hotspot, referred to as the adenine pocket. The phenyl pyrazole and the indole motif occupy the same part of the adenine pocket with

similar orientation of the corresponding N-methyl groups and the carboxamide NH setting the stage for SAR transfer between both hit series.

The medicinal chemistry challenge during hit optimization was the kinked shape of the binding pocket harboring both apolar (adenosine binding region) and polar (phosphate binding region) sites. Early synthesized analogs had the tendency to point out of the binding pocket towards the bulk water, thus showing no gain in affinity towards PHGDH. Due to more favorable physicochemical properties (low clogP, high solubility in all relevant assays) as well as the commercial availability of suitable starting materials, our initial efforts were focused on the phenylpyrazole-5-carboxamides series.

A detailed conformational analysis of the crystal structure of the screening hit **9** (K_d = 105 µM) confirmed that the observed binding confirmation is in alignment with the minimum energy confirmation induced by 1,3-allylic strain.[37, 38] The remaining proton of the cyclopropyl ring is in planar alignment with the carbonyl group of the corresponding phenylpyrazole-5-carboxamide and thus locking the conformation of the cyclopropyl moiety. Therefore, commercially available 2-methyl-5-phenyl-2*H*-pyrazole-3-carboxylic

acid (**10**) (K_d not measurable) was chosen for amide library synthesis because a clear eutomer/distomer and vectors into the phosphate channel were expected based on the key learnings from the X-ray analysis. Phenethylamides from the library such as **11** showed a potency of 22 μM in the biochemical assay, whereas the distomer **12** and the methylene analog **13** were not measureable within the detection range of up to 100 μM (Table 1).

Table 1: Effect of chiral methyl group on binding affinity.

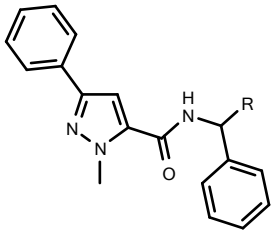

Compound	R	Biochemical PHGDH (low NAD^+) IC_{50} [μM]
(R)-11	Me	22
(S)-12	Me	> 100
13	H	> 100

To gain insight into the structure activity relationship (SAR) of the phosphate channel of PHGDH a carboxylic acid was installed in the para-position of the phenyl core thus

offering diversification opportunities. Installation of an acidic motif resulted in a dramatic boost in potency (**17**). Subsequently, these findings were independently confirmed by Frédérick *et. al.* as well as Fuller *et. al.*[29, 39] (Table 2 and Figure 2)

Having now single digit micromolar compounds in hand, it was decided to re-evaluate the contribution of the allylic strain to the binding affinity. The significant loss in potency observed with the geminal dimethyl analogue **14** illustrated the contribution of the 1,3-allylic strain to the overall binding affinity and is in good alignment with quantum mechanical geometry optimization for hydrogen atoms and the chiral methyl group at B3LYP/6-31G* level based on ligand conformation extracted from X-ray of **15** ((*R*)-pyrazolo-derivative). The R-isomer is favored by -4.35 kcal/mol over the S-isomer in the given conformation (Table 2 and Figure 6).

Table 2: The influence of allylic strain on binding affinities

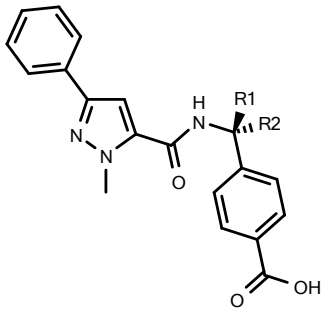

Compound	R1	R2	Biochemical PHGDH (low NAD^+) IC_{50} [μM]
14	Me	Me	1.3
15	H	Me	0.4
16	H	H	5.7
***rac*-17**	Me/H	H/Me	0.9

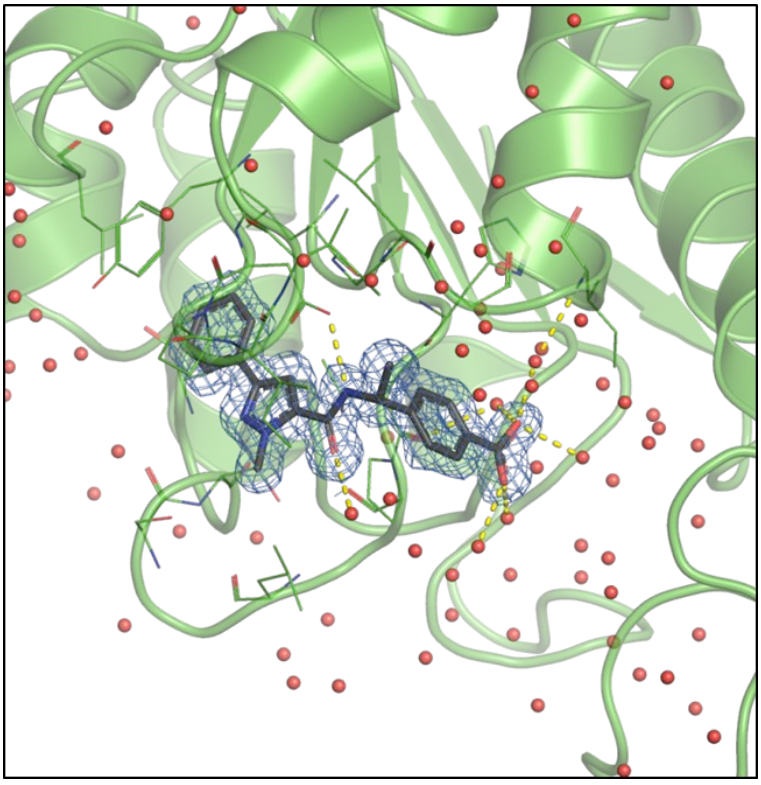

Figure 6: X-ray structure confirmation of compound **15**(PDB code: **6RJ3**).

As previously shown by Fuller *et al.*,[29] the introduction of an acidic functionality led to a > 50-fold increase in potency. Crystallographic analysis in conjunction with the biochemical assay data revealed that moving the acidic moiety away from the para position led to a significant decrease in potency. However, the para-position was also judged to be the most suitable one for further growing into the NA-site. Thus, it was

envisioned to establish appropriate replacements with additional vectors enabling building the molecule towards the substrate binding site. A summary of these efforts is shown in Table 3. Disappointingly, neither neutral, nor basic motifs resulted in the desired improvement in potency.

Table 3: Evaluation of the long range electrostatic interactions (LRE) in the phosphate channel

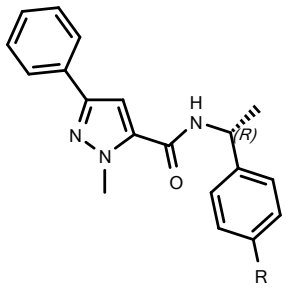

Compound	R	Biochemical PHGDH (low NAD^+) IC_{50} [µM]
15		0.4
***rac*-18**	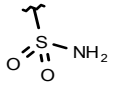	4.3
19	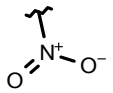	55.4
20		38.1

21	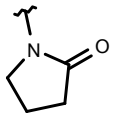	3.3
***rac*-22**		5.8
23	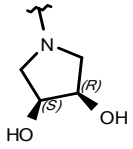	5.2
24	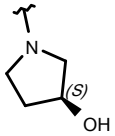	12.2
25	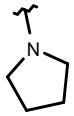	42.1
26	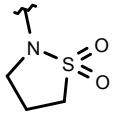	2.5
27	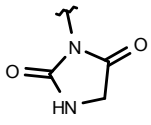	2.3
28	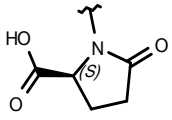	0.1

29	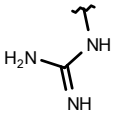	> 100
30	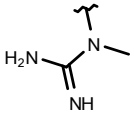	> 100
***rac*-31**	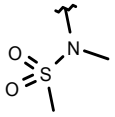	6.7
32	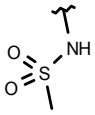	53.8
33		16.2
34	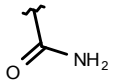	3.1
35	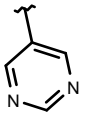	21.5
36		23.2
37		6.0
***rac*-38**		33.7

39	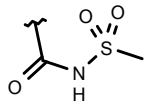	0.3
40	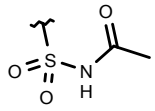	0.1
41	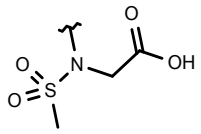	1.4
rac-**42**	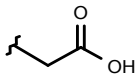	0.8

As no direct interactions between the carboxylate and the protein could be identified, long range electrostatic interactions were seen to be the most plausible explanation for the significant improvement in potency.[40] This hypothesis is further supported by the presence of multiple basic residues within a ≤ 10 Å radius around the binding site leading to a highly positively charged protein environment. Furthermore, the introduction of an acidic acyl sulfonamide **39** maintained binding affinity, again without showing direct interactions with the protein. This indicated that the exact placement of negatively charged group is of minor importance, but its presence is crucial (Figure 7).

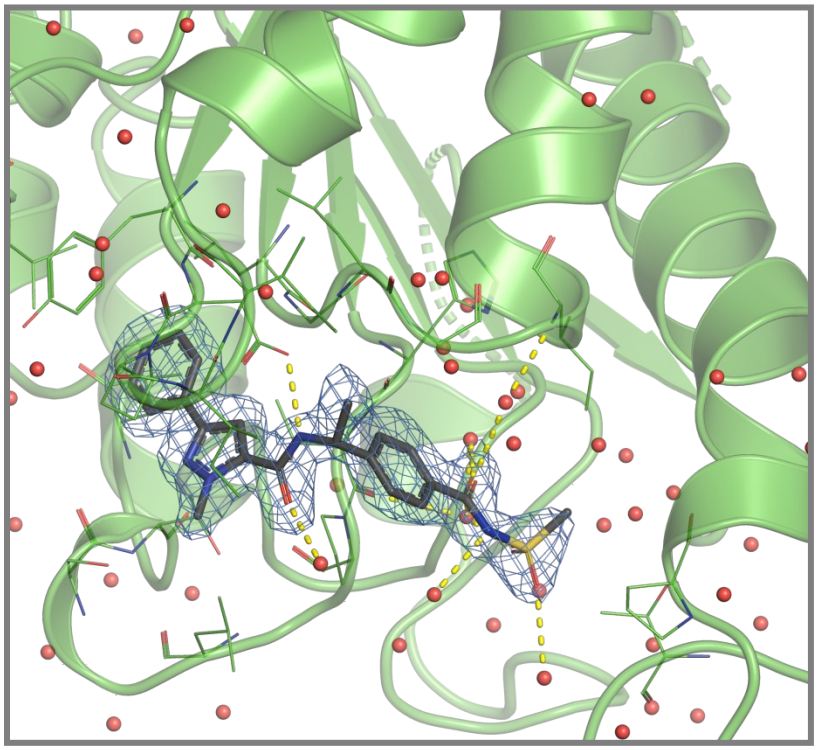

Figure 7: Long range electrostatics in PHGDHs phosphate channel exemplarily shown on acyl sulfonamide **39** (PDB code: **6RJ5**).

Inversion of the acyl sulfonamide **39** led to constitutional isomer **40**. X-ray analysis confirmed an altered binding mode, now showing an additional polar interaction with the

backbone NH of I155 (Figure 8). This combination of shape and charge led to further improvement of potency to an IC_{50} of 70 nM in the biochemical assay.

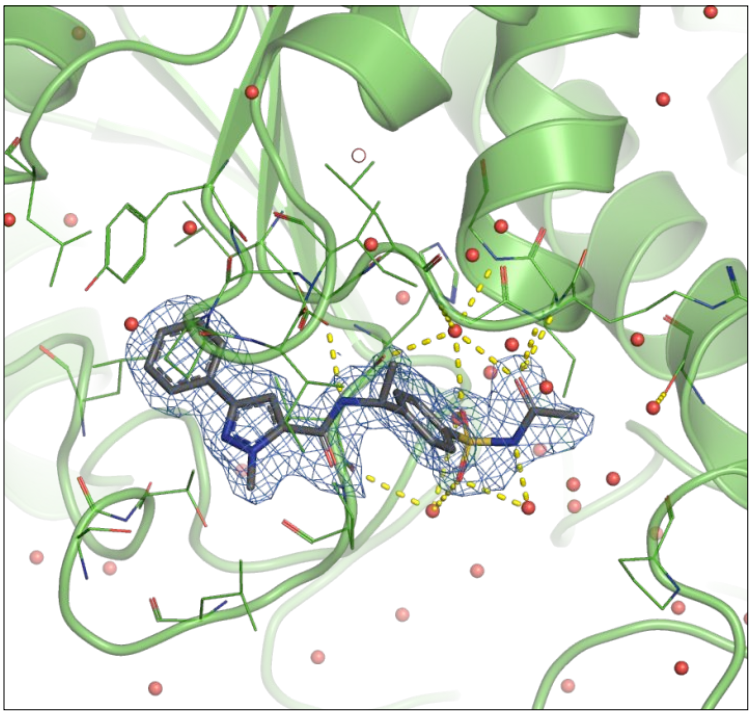

Figure 8: Addressing a new polar interaction on I155 BB-NH with kinked acyl sulfonamide **40** (PDB code: **6RJ2**)

The difference in potency of acyl sulfonamide isomers **39** and **40** indicates that shape and negative charge under physiological conditions are both crucial. The introduction of an additional kink in acyl sulfonamide **40** leads to a favorable positioning of an H-bond

acceptor enabling I155 backbone NH-interaction. Introduction of 2-(benzenesulfonyl)acetic acids (tosyl acetate) resulted in potent and highly acidic PHGDH inhibitor **43** (calc. pK_a ~ 2.5). The efforts of optimizing the interactions inside the phosphate channel by tweaking the pK_a of the acidic motif are summarized in Table 4, suggesting that the pK_a of the acid is playing a crucial role.

Table 4: Optimization of the interactions inside the phosphate channel of PHGDH

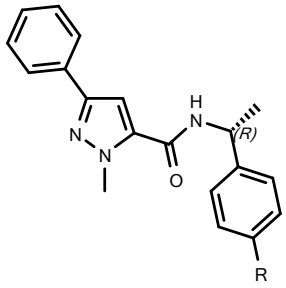

Compound	R	Biochemical PHGDH (low NAD^+) IC_{50} [nM]	calc. pK_a (most acidic)
rac-22		5,830	-
rac-40	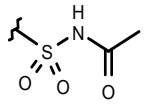	70	4.15
43	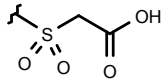	25	2.75

As previously mentioned in the screening section, a HTS was performed in parallel and identified indole-2-carboxamides as potent PHGDH inhibitors. Aniline amide **8** inhibits PHGDH with a SPR K_d of 144 µM. Applying the learnings of 1,3-allylic strain and the necessity of a negative charge of the phenylpyrazole-5-carboxamide series to the indole-2-carboxamide series resulted in compound **44** with an IC_{50} of ~ 2 µM in the biochemical driving assay. Subsequent optimization of the lipophilic interactions in the adenine pocket is illustrated in Table 5. Finally, the dichloro-dimethyl substitution pattern on the indole moiety was identified as an additional potency trigger. To be prepared for the assessment of even more potent compounds the NAD^+ concentrations were increased from 19 µM (low NAD^+) to 250 µM (high NAD^+), which shifts the IC_{50}s to 10-fold higher values (Figure 9).

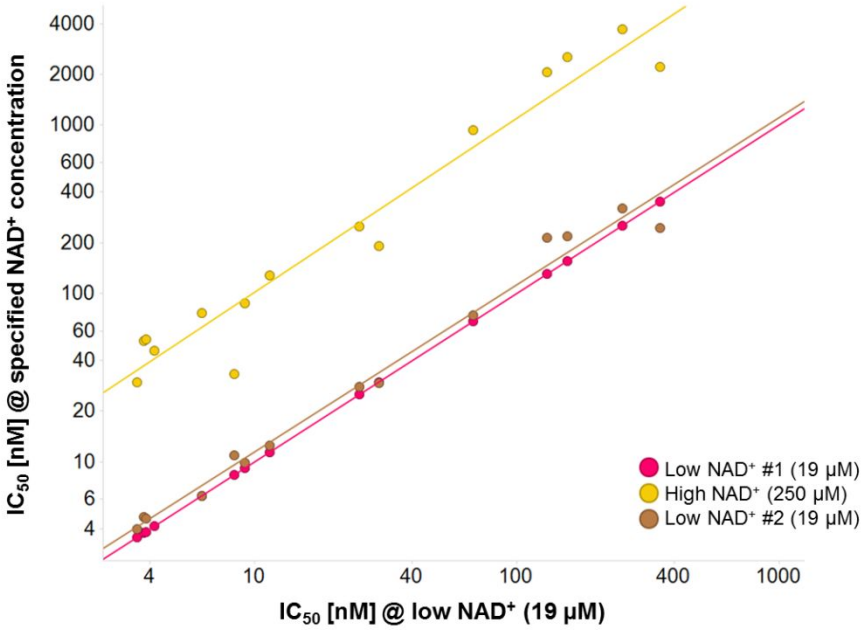

Figure 9: Assay adaption for the profiling of potent PHGDH inhibitors. Red dots depict the reference assay @19 µM NAD^+. Brown dots depict another run under the same conditions. Yellow dots indicate shifted IC_{50} values using 250 µM NAD^+.

Table 5: Optimization of the indole moiety in the adenine pocket

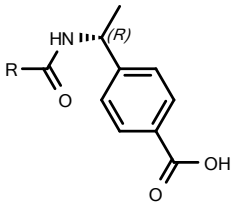

Compound	R	Biochemical PHGDH (low NAD^+) IC_{50} [nM]	Biochemical PHGDH (high NAD^+) IC_{50} [nM]
44	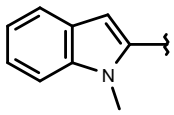	1,950	
45	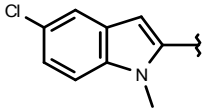	254	2,368
46	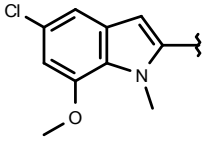	72	746

47	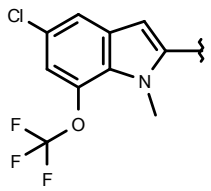	824	6,694
48	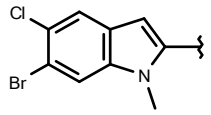	61	341
49	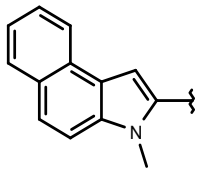	58	345
50	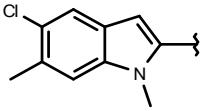	51	412
51	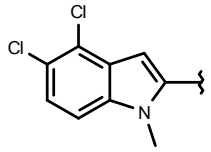	30	228
52	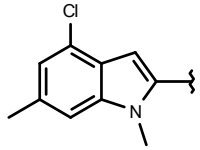	28	246
53	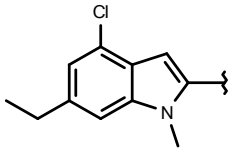	30	301

54	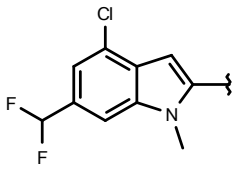	81	714
55	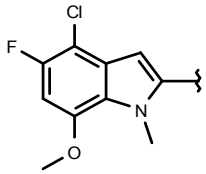	123	1,294
56	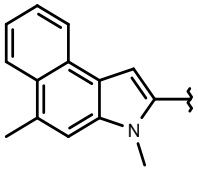	28	249
57	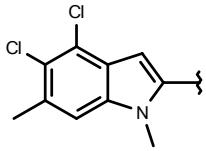	14	95

SAR transfer to the HTS derived indole-2-carboxamide series

Following identification of an optimized binder in the adenine pocket an SAR transfer from the optimization efforts in the phosphate channel was envisioned. Subsequently, tosyl acetate **58** showed an improved potency of IC_{50} = 4 nM in the adapted NAD^+ high assay and 2 nM in the NAD^+ low assay (Table 6).

Table 6: Efforts of merging of an optimized adenine pocket binder with an optimized phosphate channel binder

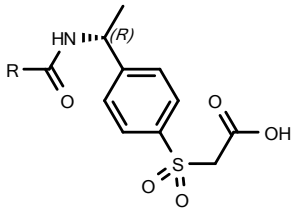

Compound	R	Biochemical PHGDH (low NAD^+) IC_{50} [nM]	Biochemical PHGDH (high NAD^+) IC_{50} [nM]
58	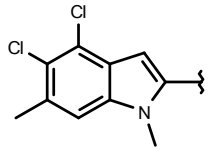	2	4
59	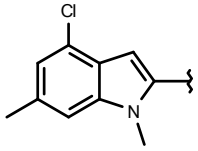	3	8

Efforts to optimize the interaction with D174

To even further improve the potency of **58** it was envisioned that an additional hydrogen bond donor (HBD) could have a chelating effect to the D174 residue of PHGDH. As the crystal structure of NAD^+/3-PG shows, two hydroxyl groups of the ribose moiety are chelating D174 (PDB code: 6CWA). Thus, it was attempted to transfer the learnings from the optimization the indole series – summarized in Table 5 – to improve the potency of fully decorated tosyl acetate **58**. Chelation as a potency driver is well described in literature and was also used by Fuller et al. for compound **1**.[29, 41] In line with this findings hydroxymethylene bearing compound **BI-4924** showed an even further improved IC_{50} of ≤3 nM, which again is believed to hit the assay-wall. Poor cell membrane permeability and a high efflux ratio (as judged by the industry standard assay CaCo-2) were identified as the main reasons for the high gap between the nanomolar potency in the biochemical assay and the moderate intracellular biomarker modulation in the micromolar range. An X-ray analysis of the binding mode is depicted in Figure 10.

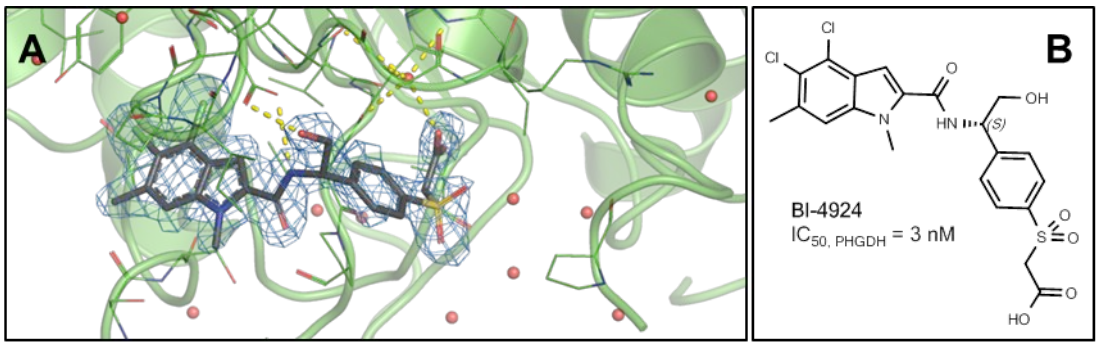

C		BI-4924		
IC_{50}; NAD^+ high assay (250 µM)	[nM]	3		
IC_{50}; ^{13}C-Serine; 72 h	[nM]	2,200		
Cerep panel > 50% inhibition @10 µM		4/40		
Solubility pH 4.5 | 6.8	[mg/mL]	64	59	
Microsomal Stab. m | r | h	[%Q_H]	< 23	< 24	< 24
Hepatocytic Stab. m (0% | 50% serum)	[%Q_H]	38	26	
CaCo-2 ab-ba average | ratio	[10^{-6} cm/s] | -	0.2	11	
Plasma Protein Binding 10% FCS | m	[%]	83	99.6	

Figure 10: (A) Binding mode of **BI-4924** (PDB code: **6RJ6**); (B) Chemical structure of **BI-4924**; (C) additional *in vitro* data for **BI-4924**; m = murine, r = rat, h = human; CaCo-2 permability: ab = apical – basolateral permeation / transport, ba = basolateral – apical permeation / transport; FCS = fetal calf serum

As further elaborated in Table 7, neither the additional acidification of the hydroxyl group nor changing the nature of the HBD resulted in improved binding affinities.

Table 7: Optimization of the bidentate D174 interaction

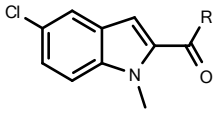

Compound	R	Biochemical PHGDH (low NAD^+) IC_{50} [µM]
rac-60	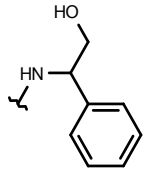	5.20
rac-61	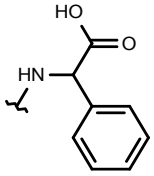	> 100
rac-62	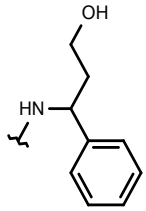	100

rac-63	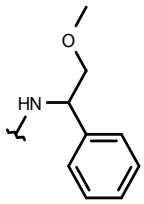	> 100
rac-64	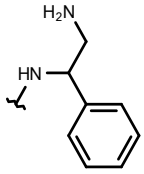	39.6
rac-65	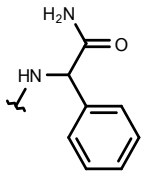	> 100
66	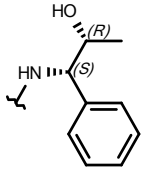	12.1
67	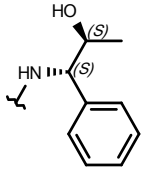	11.7
68	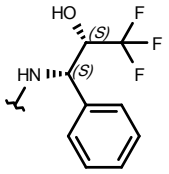	> 100

69	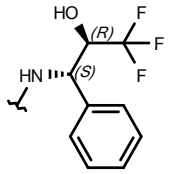	> 100

The compounds were then evaluated for cellular activity. Effects of the compounds on the production of [^{13}C]-serine, upon feeding of uniformly labeled [^{13}C]-glucose, was measured by mass spectroscopy (detailed protocol: see supporting information). Given the low pK_a of the acidic moiety it was not surprising that the permeability in CaCo-2 cells of **BI-4924** is low (0.2 *10^{-6}cm/sec). This leads to a significant off-set between the biochemical IC_{50} values and IC_{50} values measured for the cellular biomarker modulation (3 nM biochemical IC_{50} vs. 2.2 µM IC_{50} in serine modulation).

Selectivity profiling

To gain a better understanding of the binding selectivity of our PHGDH inhibitors we synthesized two derivatives of **BI-4924**, compound **70** and compound **71**, each bearing

a primary amine attached via a spacer to two distinct parts of the molecule. These PHGDH binders were immobilized on NHS-activated Sepharose via amide formation and incubated with MDA-MB-468 cell extracts in the presence or absence of 10 μM **BI-4924**. Identification and quantitative comparison of the Sepharose-bound protein fraction by Trypsin digestion and LC-MS/MS analysis revealed a clean selectivity profile for **BI-4924**. Of 31 dehydrogenase in the dataset, only alcohol dehydrogenase class-3 (ADHX) and 3-hydroxyisobutyrate dehydrogenase (3HIDH) were identified as off-targets (Figure 11 and Supplemental Material).

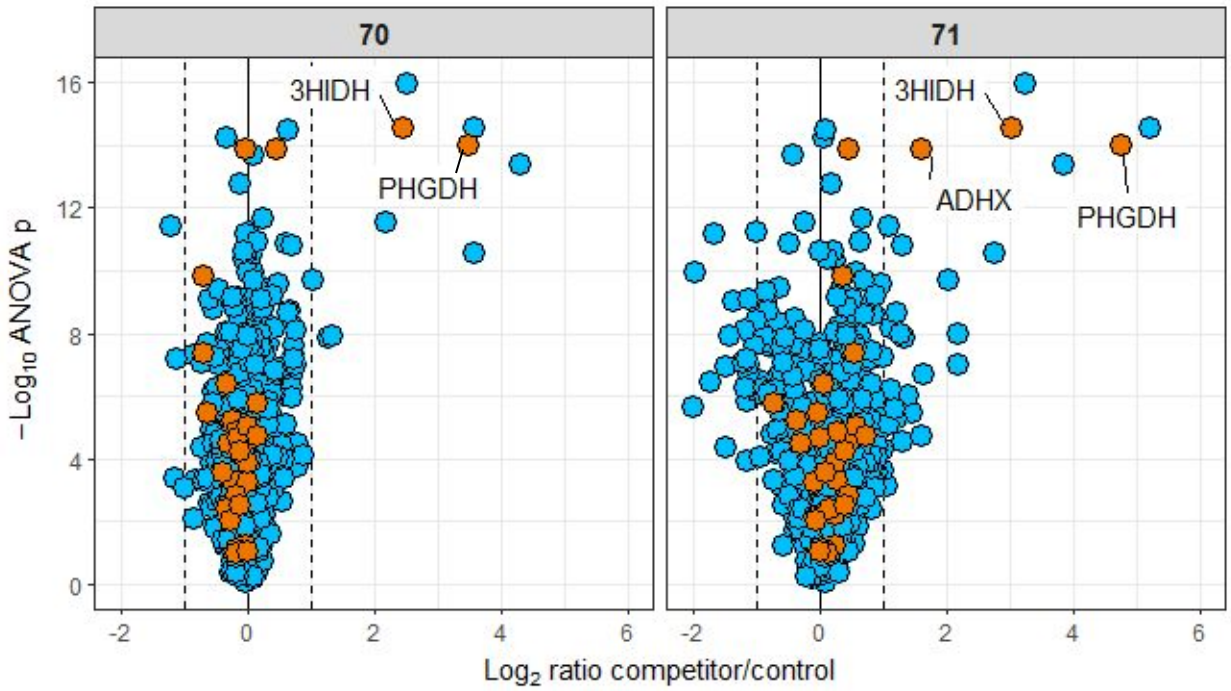

Figure 11: Selectivity profile of **BI-4924** obtained by quantitative chemical proteomics. Proteins (orange dots, dehydrogenases; blue dots, other proteins) from of MDA-MB-468 cell are displaced from the compound **70** or **71** affinity matrices by 10 μM competing **BI-4924** specifically (versus DMSO control) and significantly. Data plotted log2 of the fold change versus DMSO control against –log10 of the P value per protein (ANOVA, N = 3). All t-tests performed were two-tailed t-tests assuming equal variances.

Cellular uptake

In order to overcome the inherent low permeability of the acid **BI-4924** and compensate against high intracellular NADH/NAD^+ levels (~ 0.3 mM) we hypothesized that intracellular ester cleavage of a permeable ester containing PHGDH prodrug would liberate the corresponding active carboxylic acid and, due to its poor permeability, lead to an accumulation of the acid inside cells. Thus, cellular uptake studies were performed in MDA-MB-468 cells to better understand these findings. After defined intervals, following treatment with ethyl ester **BI-4916,** MDA-MB-468 cells were harvested, and the concentrations of both the ester and the carboxylic acid were determined in the medium, as well as intracellularly. An analogous experiment was performed with the addition of **BI-4924** to the medium. Thus it could be shown that **BI-4924** is up to 140-fold enriched inside the cells in a time dependent manner after addition of **BI-4916** versus **BI-4924** to the medium (Figure 12). This accumulation can be explained by differences of permeability between prodrug and acid and efficient conversion of prodrug into acid inside the cells. Simultaneously, the prodrug compound also gets cleaved in the medium, resulting again in an impermeable acid negligibly contributing to the intracellular drug levels (see supplementary). This medium instability is in good

agreement with the ester's stability in plasma protein containing media: 10% FCS $t_{(1/2)}$ = 276 min; mouse serum $t_{(1/2)}$ = 135 min. Finally, after complete conversion of the prodrug, the compound concentrations between cell and medium equilibrate and the accumulation factor approaches unity after approximately 72 h. Using an AUC based approach an average accumulation factor of 23.4 over a time period of 72 h can be calculated (grey dashed line, Figure 12).

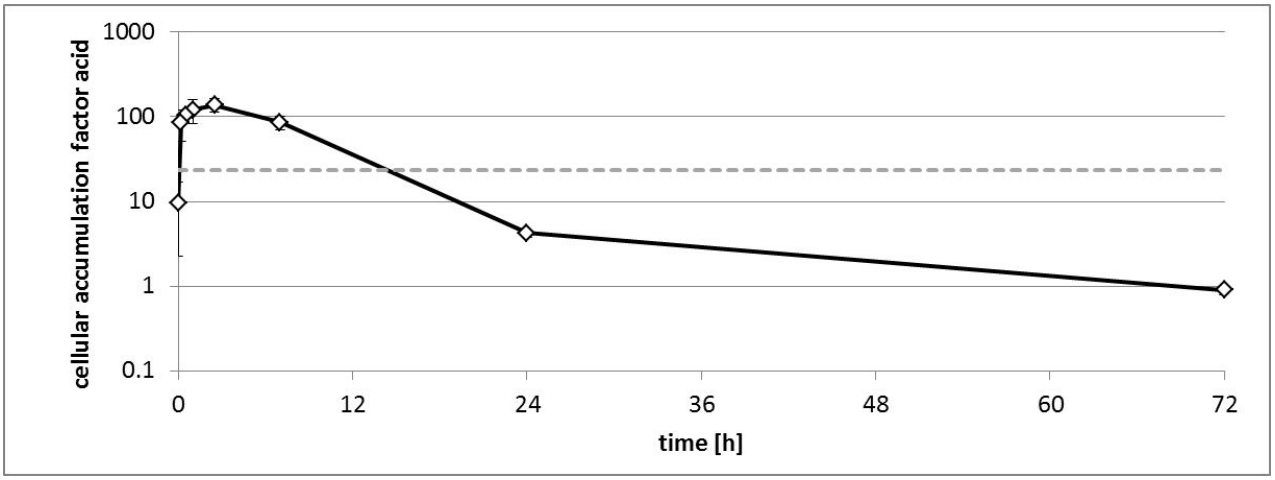

Figure 12: Ratio of mean cellular concentrations of acid **BI-4924** (black diamonds) at various time points after the addition of 3 µM ester **BI-4916** versus 3 µM acid **BI-4924** into the medium. Error bars indicate the Standard Gaussian Error calculated from the standard deviations of the individual assays. The grey dashed line indicates the average accumulation factor for a time period of 72 h.

Biomarker Modulation

As a next step we envisioned to measure the cellular enrichment in a pathway relevant manner to establish an *in vitro* PK/PD relationship. Therefore, a cellular target engagement study in disease relevant MDA-MB-468 TNBC-cells was set up using uniformly labeled ^{13}C-glucose as a substrate. Being metabolized according to Figure 1 the MS-based quantification of ^{13}C-serine served as readout. Indeed, treatment of MDA-

MB-468 cells with ethyl ester **BI-4916** resulted in a ~70-fold improved transient modulation of ^{13}C-derived serine (measured "IC_{50}" = 29 nM@1 h; IC_{50} = 2,000 nM@72 h) compared to the application of **BI-4924**. This is in good agreement with the above mentioned time dependent enrichment factor and shows that CaCo-2 efflux does not seem to be predictive for MDA-MB-468 cells.

CONCLUSIONS

Herein we report the discovery of the highly potent and selective PHGDH inhibitor **BI-4924** and its ester prodrug **BI-4916**. Based on the combined efforts of an HTS campaign as well as a fragment based finding campaign, a ~100 µM screening hit was optimized to single digit nM potency by means of structure based drug design (SBDD). In a nutshell, compound **BI-4924** gains its binding affinity by a strong lipophilic interaction in the adenine pocket, accompanied by a bidentate polar anchor interaction of a secondary amide and a hydroxyl group with D174. Following the kink introduced by 1,3-allylic strain, a tosyl acetate finally places the required negatively charged acidic moiety

in the right position to interact with a backbone NH of I155 and the surrounding arginine as well as histidine side chains by means of LRE (Figure 10A). Compound **BI-4924** is a lipophilic, highly plasma protein bound PHGDH inhibitor with excellent microsomal, as well as hepatocytic stability (Figure 10C). The low pK_a of the compound leads to excellent aqueous solubility over a broad pH-range. Furthermore, **BI-4924** exhibits an excellent selectivity profile as shown by chemical proteomics (2/31 dehydrogenases) as well as in a CEREP counter screen panel (4/40 off targets > 50% inhibition @ 10µM; see supplementary information).

The interconversion of **BI-4924** to its ester prodrug **BI-4916** increased cell penetration and thus led to a transient accumulation of **BI-4924** inside the cells thereby generating an *in vivo*-like intracellular concentration-time-profile for **BI-4924** *in vitro*. In agreement with a transient intracellular compound accumulation, a time-dependent double digit nanomolar modulation of the ^{13}C-serine flux could be observed. The intrinsic instability in presence of esterases disqualified **BI-4916** as an *in vivo* tool. However, we are convinced that both **BI-4924** and **BI-4916** will serve as valuable *in vitro* tools to further explore yet unknown aspects of PHGDH inhibition.

EXPERIMENTAL SECTION

Biochemical Assays

HTS PHGDH Inhibitor Assay. To 100 nL of test compounds (10 mM in DMSO) in white Greiner low volume plates are added 5 µL of enzyme working solution (200 mM Tris-HCl, pH 7.4/1 mM EDTA/2 µM NAD/0.02% Tween20. The buffer is supplemented with 400 ng/mL PHGDH (construct corresponding to pdb id 2G76. Amino acids 4-315, N-terminal HIS-tag, TEV cleavage site. Plasmid from SGC.) (prior to the assay). Each assay plate contains 16 wells with NAD alone a as high control. 1 µL of AuCl3 (50 mM in DMSO) is added to column 24 as a low control. 5 µL of substrate solution (the Promega bioluminescent NADH detection kit (#V865A) is supplemented with Promega substrate 1 (Proluciferin), promega enzyme 1 (Diaphorase) and 3-phosphoglycerate (280 mM stock) in the ratio (parts): 200/1/1/5 is added to each well and the plates are then incubated for 2 h at RT. Measurement is done with an EnVision (luminescence measurement, optimized for shortest reading time per well without performance loss).

Calculation: Signal for unknown compounds was normalised using high and low control wells as follows: %activity = ((RFU(sample)-RFU(low))/((RFU(high)-RFU(low)))*100. An inhibitor of the PHGDH enzyme will give values lower than 100 %CTL.

Diaphorase NADH counterscreen ("Shortcut assay"). To 100 nL of test compounds (10 mM in DMSO) in white Greiner low volume plates are added 5µL of assay buffer solution (200 mM Tris-HCl, pH 7.4/1 mM EDTA/1 µ M NADH/0.02% Tween20). Each assay plate contains 16 wells with assay buffer solution alone a as high control. 1µL of AuCl3 (50 mM in DMSO) is added to column 24 as a low control. 5 µL of substrate solution (the Promega bioluminescent NADH detection kit (#V865A) is supplemented with Promega substrate 1 (Proluciferin), promega enzyme 1 (Diaphorase) and 3-phosphoglycerate (280 mM stock) in the ratio (parts): 200/1/1/5 is added to each well and the plates are then incubated for 2 h at RT. Measurement is done with an EnVision (luminescence measurement, optimized for shortest reading time per well without performance loss). Calculation: Signal for unknown compounds was normalised using high and low control wells as follows: %activity = ((RFU(sample)-

RFU(low))/((RFU(high)-RFU(low)))*100. An inhibitor of the Diaphorase/Proluciferin/Luciferase will give values lower than 100 %CTL.

3-Phosphoglycerate dehydrogenase (PHGDH) fluorescence intensity assay. This assay is used to identify compounds which inhibit the enzymatic activity of PHGDH which catalyzes the reaction of 3-phosphoglycerate (3-PG) and NAD to 3-phosphohydroxypyruvate and NADH. The produced NADH is used in a coupled reaction for diaphorase mediated reduction of resazurin to resorufin which can be measured in fluorescence intensity readout. The full length version of PHGDH enzyme was expressed in E. coli with an N-terminal HIS-tag and a TEV cleavage site. The 3-phosphoglycerate substrate was purchased from Sigma. NAD, diaphorase and resazurin were purchased from Sigma Aldrich. Compounds are dispensed onto assay plates (black, low volume, flat bottom 384 well, Corning) using an Access Labcyte Workstation with the Labcyte Echo 55x from a DMSO compound stock solution. For the highest assay concentration of 100 µM, 150 nL of compound solution are transferred from a 10 mM DMSO compound stock solution. A series of 11 concentrations is

transferred for each compound at which each concentration is fivefold lower than the previous one. DMSO is added such that every well has a total of 150 nL compound solution. The assay has been performed at two different NAD/3-PG ratios (final assay concentrations): NAD low: 18.8 µM NAD/175 µM 3-PG; NAD high: 250 µM NAD/500 µM 3-PG. 5 µl of PHGDH protein (final assay concentration 100 ng/ml) in assay buffer (125mM Tris-HCl, pH 7.5; 56.25 mM hydrazine sulfate pH 9.0; 2.5 mM EDTA; assay specific NAD concentration; 0.0125% Tween20) are added to the 150 nL of transferred compound stock solution. 10 µl of a mix containing assay specific 3-PG concentration, resazurin (25 µM final assay concentration) and diaphorase (35 µg/ml final assay concentration) are added. Plates are kept at room temperature. After 240 minutes incubation time the fluorescence signal is measured in a PerkinElmer Envision HTS Multilabel Reader with an excitation wavelength at 530 - 560nm and an emission wavelength at 590 nm. Each plate contains negative controls (diluted DMSO instead of test compound; reaction as described with PHGDH protein) and positive controls (diluted DMSO instead of test compound; reaction as described with buffer instead of PHGDH protein). Negative and positive control values are used for normalization. An

internal standard was used and IC50 values are calculated and analysed using a 4 parametric logistic model.

Cellular Assays

^{13}C Serine Assay in MDA-MB-468 Cells. MDA-MB-468 cells (5000/well) in medium (DMEM glucose free (Gibco # A14430-01) with 10% FCS (Gibco # 26140), Na-Pyruvate (Gibco # 11360) and Glutamax I (Gibco # 35050), 90 µL/well) were seeded into a 96 well plate and incubated at 37 °C in a CO2 incubator overnight. Test compounds were serially diluted (8 dilution steps (1:3)) in medium in duplicates, and 10 µl of this dilutions were added to the cell culture (final DMSO concentration 1%). After an incubation at 37 °C in a CO2 incubator for 1 h, 24 h, and 72 h respectively, 20 mM 13C glucose (Aldrich # 389374) in medium (50 µl) was added per well. After 180 minutes incubation at 37 °C in a CO2 incubator 150 µl methanol (20% H2O, -80 °C) was added, and the plates were sealed immediately and frozen at -80 °C. At day of measurement plates were thawn, centrifuged and the supernatant evaporated. The samples were re-suspended in 100 µl water for tandem mass spectrometry. 13C serine levels were

analyzed with LC/MS/MS using Multiple Reaction Monitoring (MRM). Data Analysis: Detected Peak Areas with MRM transition 107.090/75.80 Da were integrated using Analyst software. IC50 values were calculated from these values using a 4 parametric logistic model.

Uptake-Assay. 200,000 cells per well were seeded onto 6-well plates and incubated overnight at 37 °C in 3 ml incubation medium (DMEM (Lonza # 12-604F); 10 % FCS (HyClone FBS Thermo Fisher #SH3007103)) before starting the incubation. Then, 9 µl of a 1mM DMSO stock was added to the incubation, yielding a 3 µM concentration of test compound in the supernatant at the beginning of the incubation. The experiment was stopped at various time points after the compound was added: 0 min, 10 min, 30 min. 60 min, 150 min, 7 h, 24 h, 72 h. At each time point the supernatant was taken and frozen to -80 °C. Cells were washed 3x with 1 mL of ice cold PBS buffer (Ca/Mg free Gibco # 14200-067)) for 1 min each. While the first 2 washes were discarded, the third wash was taken and frozen to -80 °C to check the efficiency of the washing procedure. Cells were lysed with 500 µl of 80:20 Acetonitrile/Water and frozen to -80 °C. All

samples were quantified via HPLC-MS-MS using calibration curves for the ester and the corresponding acid for absolute quantification of time-dependent intracellular and extracellular concentrations. A 12 point calibration curve was generated with 50% acetonitrile/water. Samples were prepared accordingly. An internal standard was used for exact quantification. Samples were measured on a SCIEX QTRAP 4000 System and analysed using the Analyst® software.

(Bio)Physical Methods

PHGDH SPR Assay. Immobilization of target protein: PHGDH (construct corresponding to pdb id 2G76. Amino acids 4-315, N-terminal HIS-tag, TEV cleavage site. Plasmid from SGC.) is immobilized on an CM5 chip (GE). The surface is activated with EDC/NHS with a contact time of 540 s. The protein is diluted in NaAc (pH 5.0) + 0.5 mM TCEP. A protein immobilization level of 1000 - 6000 response units is achieved. For immobilization we use 10mM HBS-EP+ pH 7.4 (GE) + 0.5 mM TCEP as a running buffer. This process is performed at 20 °C. Interaction experiments: All interaction experiments are performed at 20 °C in Tris(hydroxymethyl)aminomethane 50 mM, NaCl

150 mM, TCEP 0.5 mM, EDTA 1 mM, Tween20 0.02%, DMSO 1% - 5% (v/v), pH 7.4. The compounds are diluted in the running buffer and injected at a flow rate of 30 µl/min over the immobilized target protein. Data analysis: Sensorgrams from reference surfaces and blank injections are subtracted from the raw data prior to data analysis, using Biacore T200 evaluation software. Sensorgrams recorded at different compound concentrations in multi-cycle experiments are fitted using a 1:1 interaction model, with a term for mass-transport included.

LDH SPR Assay. Immobilization of target protein: Lactate Dehydrogenase chicken heart, recombinant from E.Coli (Sigma Aldrich, CAS Nr. 9001-60-9, order number 59747) is immobilized on a CM5 chip (GE). The surface is activated with EDC/NHS with a contact time of 540 s. The protein is diluted in NaAc (pH 5.5). A protein immobilization level of 1000 - 6000 response units is achieved. For immobilization we use 10 mM HBS-EP+ pH 7.4 (GE) + 0.5 mM TCEP as a running buffer. This process is performed at 20 °C. Interaction experiments and Data analysis is done as described for the PHGDH SPR Assay

CAII SPR Assay. Immobilization of target protein: Carbonic Anhydrase II (Sigma Aldrich) is immobilized on a CM5 chip (GE). The surface is activated with EDC/NHS with a contact time of 540 s. The protein is diluted in NaAc (pH 5.0) + 0.5 mM TCEP. A protein immobilization level of 1000 - 6000 response units is achieved. For immobilization we use 10 mM HBS-EP+ pH 7.4 (GE) + 0.5 mM TCEP as a running buffer. This process is performed at 20 °C. Interaction experiments and Data analysis is done as described for the PHGDH SPR Assay.

Metal salts: ICP-MS method. Metal impurity determination from DMSO stock solutions. This method is designed to quantify metal impurities that are included in DMSO stock solutions as obtained from the respective dispensaries. No effort is made to bring insoluble metal components into solution, as we are only interested in soluble components that potentially interfere with biophysical or biochemical assays. The intended final compound concentration is approx. 0.2 µM which is obtained as follows. 25 µl 10 mM DMSO stock solution (or equivalent) are ordered and diluted with 235 µL DMSO, 65µL Internal Standard solution (in most cases Indium) and 975 µL of a freshly

prepared 2% HNO_3 solution yielding a total of 1300 µL that can be used for analysis. If compound precipitates the solution is filtered through a 0.45 µm cellulose filter. Data is evaluated with Mass Hunter software and quantitation of the individual metals is obtained from calibration curves obtained on the same day with Indium or Gallium as internal control standard. The threshold of quantitation for each element depends on how well it can be detected by ICPMS and its natural occurrence as a ubiquitous contaminant in our setup. This value is represented in background equivalent concentrations (BEC) and was determined for our specific setup for each metal reported below. The metal contaminants are reported in mol percent relative to the compound, if they exceed the thresholds shown below, otherwise they are reported as <0.XX mol%. Mg < 0.40; Al < 0.10; Mn < 0.01; Fe < 0.01; Co < 0.01; Ni < 0.01; Cu < 0.02; Zn < 0.02; Ru < 0.01; Rh < 0.01; Pd < 0.01; Ag < 0.01; Cd < 0.01; Sn < 0.01; Cs < 0.01; Au < 0.01.

NMR. NMR experiments were recorded on Bruker Avance HD 400 MHz and 500 MHz spectrometers equipped with BBO Prodigy and TCI cryoprobes at 298 K, respectively. Samples were dissolved in 600 µL DMSO-d_6 and TMS was added as an internal

standard. 1D 1H spectra were acquired with 30° excitation pulses and an interpulse delay of 4.2 sec with 64k data points and 20 ppm sweep width. 1D ^{13}C spectra were acquired with broadband composite pulse decoupling (WALTZ16) and an interpulse delay of 3.3 sec with 64 k data points and a sweep width of 240 ppm. Processing and analysis of 1D spectra was performed with Bruker Topspin 3.2 software. No zero filling was performed and spectra were manually integrated after automatic baseline correction. Chemical shifts are reported in ppm on the δ scale. HSQC spectra were recorded on all samples to aid the interpretation of the data and to identify signals hidden underneath solvent peaks. Spectra were acquired with sweep widths obtained by automatic sweep width detection from 1D reference spectra in the direct dimension with 1k datapoints and with 210 ppm and 256 datapoints in the indirect dimension.

Protein-Science

PHGDH Expression. A vector coding for PHGDH (A4-V315) with an N-terminal 6xHis-tag and a TEV cleavage site was obtained from the Structural Genomics Consortium

(SGC). Recombinant PHGDH was expressed in E. coli BL21(DE3) at 18°C overnight in 2x YT medium (Sigma).

PHGDH Purification. Cell pellets were re-suspended in 50 mM NaH_2PO_4, 0.3 M NaCl, 10 mM imidazole, 0.5 mM TCEP containing protease inhibitor cocktail (COMPLETE without EDTA, Merck) according to manufacturer specifications. Cells were broken by sonication at 4 °C. A 50% PEI solution was added to a final concentration of 0.15% (v/v) and stirred for 30 minutes on ice followed by centrifugation at 26,000xg for 45 minutes at 4 °C. The supernatant was applied to a NiNTA column (HisTrap, GE Healthcare) in buffer A (50 mM NaH_2PO_4, 0.3 M NaCl, 10 mM imidazole, 0.5 mM TCEP), washed with buffer A containing 50 mM imidazole and eluted with a gradient to buffer A containing 0.25 M imidazole. Fractions containing PHGDH were pooled and the His-tag was cleaved off by incubation with TEV protease at 4 °C overnight. PHGDH was further purified by gel filtration (HiLoad Superdex S75, GE Healthcare) equilibrated in 10 mM HEPES, 500 mM NaCl, 5% glycerol, 0.5 mM TCEP, pH 7.5

Removal of NAD^+. Activated charcoal powder (extra pure, Merck) was washed twice with water followed by ethanol and finally with 0.1 M HEPES buffer pH 7.5. The first 2 washing steps were performed in a small spin column (BioRad) to remove fines. A small amount (> 2x the estimated mass of PHGDH in solution) of washed charcoal was added to the PHGDH solution. The suspension was put on a spinning wheel and rotated overnight at 4 °C. Charcoal was removed by centrifugation and/or filtration. Removal of NAD+ was monitored at 322 and 260 nm. PHGDH was finally concentrated to ~15 mg/ml in centrifugal concentrator (BioMax) using a 10k cutoff membrane and stored at –80 °C.

Chemical Proteomics. Cell pellets were lysed in 20 mM HEPES pH 7.5, 150 mM KCl, 1% Triton X-100 and cleared at 30,000 x g. The affinity matrices with compounds 70 and 71 were prepared by amide formation with Magnetic NHS Sepharose (GE Healthcare) in DMSO/TEA to a ligand density of 10%. Cell extract and 200 nL affinity matrix were incubated in the presence of 10 µM BI-4924 or DMSO. After 2h incubation, the matrices were washed and bound proteins were proteolytically eluted using Trypsin

(Pierce) in the presence of 5 mM TCEP and 10 mM 2-chloroacetamide. Peptides were purified by solid-phase extraction (Sep-Pak tC18, Waters) and analyzed on a nanoflow-LC system (Thermo Fisher) hyphenated to a Q-Exactive Plus mass spectrometer (Thermo Fisher). Spectra were assigned using Mascot (Matrix Science) and label-free quantification was perfomed using Progenesis QI (Waters).

Protein crystallization. Protein crystallization was done with the hanging drop method by incubating PHDGH (12 mg/mL in 25 mM HEPES pH 7.5, 300 mM NaCl, 0.5 mM TCEP) with the ligand (100 mM DMSO stock solution, final concentration 1 mM) for 1 hour. 1 µL of protein solution was mixed with 1 µL of reservoir solution (25 % PEG 8000, 100 mM MES pH 6.6, 200 mM lithium sulfate, 4 mM DTT) at 4 °C. Crystals were frozen in liquid nitrogen and data were collected at the SLS beam line X06SA (Swiss Light Source, Paul Scherrer Institute) at a wavelength of 1 Å using the PILATUS 6M detector. The crystals belonged to space group P21 and contained 2 monomers per asymmetric unit. Images were processed with autoPROC.[42] The resolution limits were set using default autoPROC settings. The structures were solved by molecular

replacement using the PHGDH structure 2G76 as a search model. Subsequent model building and refinement was done using standard protocols using CCP4,[43] COOT,[44] and autoBUSTER.[45] Statistics for data collection and refinement can be found in tables in the supporting information. Crystallographic work for the 3-PG structure was done by Beryllium Discovery (Bedford, MA). The coordinates and structure factors have been deposited at the Protein Data Bank with the accession code 6CWA (**3-PG**), 6RJ6 (**BI-4924**), 6RJ3 (**15**), 6RJ2 (**40**), 6RJ5 (**39**) and 6RIH (**9**).

Syntheses of Compounds.

General Section: All samples showed a purity of ≥95%. HPLC traces of selected compounds are available as supporting information. Samples were analyzed on an Agilent 1200 series LC system coupled with an Agilent 6140 mass spectrometer. Purity was determined via UV detection with a bandwidth of 170nm in the range from 230-400nm. LC parameters were as follows: Waters Xbridge C18 column, 2.5µm particle size, 2.1 x 20mm or 3.5µm particle size, 2.1 x 30mm, respectively. Run time 2.1 minutes, flow 1ml/min, column temperature 60°C and 5µl injections. Solvent A (20mM

NH_4HCO_3/ NH_3; pH 9), solvent B (MS grade acetonitrile). Start 10% B, gradient 10% - 95% B from 0.0 - 1.5min, 95% B from 1.5 - 2.0min, gradient 95% - 10% B from 2.0 – 2.1min.

Synthetic Procedures

3-[(1-Methyl-1H-indole-2-carbonyl)-amino]-benzoic acid methyl ester (Int-01). **General Method A**. To 1-methylindole-2-carboxylic acid (50 mg, 0.28 mmol) and HATU (163 mg, 0.42 mmol) in dry DMSO (300 µL) iPr_2NEt (135 µL, 0.84 mmol) was added and stirred for 5 min at room temperature. Methyl 3-aminobenzoate (51 mg, 0.34 mmol) was added and stirred for 1.5 h. The reaction mixture was partitioned between water and EtOAc, and the organic layer was washed with water and saturated aqueous NaCl solution. The organic layer was dried (Na_2SO_4) and concentrated in vacuo to give crude **Int-01** in 78 mg (90%) yield, which was used in the next step without further purification.

3-[(1-Methyl-1H-indole-2-carbonyl)-amino]-benzoic acid (8). **General Method B**. 3-[(1-Methyl-1H-indole-2-carbonyl)-amino]-benzoic acid methyl ester (**Int-01**) (77 mg, 0.25 mmol) in MeOH (0.5 mL) was treated with 8 N aqueous NaOH (0.2 mL) and stirred for 1

h at 80 °C. The mixture was concentrated in vacuo, and the residue was dissolved in DMSO. The reaction mixture was filtered and purified by prep. HPLC (MeCN/water) to give **8** as a white solid in 54 mg (73%) yield. ^{1}H NMR (500 MHz, DMSO-d_6) δ 10.48 (s, 1H), 8.44 (s, 1H), 8.01 (br d, J=8.20 Hz, 1H), 7.69 (s, 2H), 7.58 (d, J=8.51 Hz, 1H), 7.47 (t, J=7.88 Hz, 1H), 7.37 (s, 1H), 7.32 (t, J=7.57 Hz, 1H), 7.14 (t, J=7.41 Hz, 1H), 4.02 (s, 3H), COOH not visible. ^{13}C NMR (125 MHz, DMSO-d_6) δ 167.4, 160.7, 139.2, 138.8, 131.8, 131.8, 128.9, 125.5, 124.4, 124.1, 124.1, 121.9, 121.0, 120.4, 110.7, 105.9, 31.5. HRMS (m/z): $[M+H]^+$ calcd. for $C_{17}H_{14}N_2O_3$, 295.10772; found, 295.10797. HPLC Rt = 0.82.

2-Methyl-5-phenyl-2H-pyrazole-3-carboxylic acid cyclopropylamide (9). The title compound was prepared according to General Method A from 2-methyl-5-phenyl-2H-pyrazole-3-carboxylic acid (600 mg, 2.97 mmol) in 630 mg yield (88%). ^{1}H NMR (400 MHz, DMSO-d_6) δ 8.52 (br s, 1H), 7.74 (br d, J=7.10 Hz, 2H), 7.42 (t, J=7.10 Hz, 2H), 7.32 (br t, J=7.10 Hz, 1H), 7.20 (br s, 1H), 4.09 (br s, 3H), 2.82 (br s, 1H), 0.65-0.80 (m, 2H), 0.58 (br s, 2H). ^{13}C NMR (100 MHz, DMSO-d_6) δ 160.4, 148.1, 136.8, 132.6,

128.8, 127.8, 124.9, 104.1, 39.9, 22.6, 5.7. HRMS (m/z): $[M+H]^+$ calcd. for $C_{14}H_{15}N_3O$, 242.12879; found, 242.12900. HPLC Rt = 1.07.

2-Methyl-5-phenyl-2H-pyrazole-3-carboxylic acid ((R)-1-phenyl-ethyl)-amide (11). The title compound was prepared according to General Method A from 2-methyl-5-phenyl-2H-pyrazole-3-carboxylic acid (25 mg, 0.12 mmol) in 32 mg (84%) yield. ^{1}H NMR (500 MHz, DMSO-d_6) δ 8.87 (br d, J=7.88 Hz, 1H), 7.78 (br d, J=7.25 Hz, 2H), 7.37-7.49 (m, 5H), 7.28-7.37 (m, 3H), 7.20-7.28 (m, 1H), 5.14 (quin, J=7.01 Hz, 1H), 4.06 (s, 3H), 1.48 (br d, J=6.94 Hz, 3H). ^{13}C NMR (125 MHz, DMSO-d_6) δ 158.5, 148.1, 144.4, 136.8, 132.6, 128.8, 128.3, 127.8, 126.8, 126.1, 124.9, 104.3, 48.1, 39.0, 22.2. HRMS (m/z): $[M+H]^+$ calcd. for $C_{19}H_{19}N_3O$, 306.16009; found, 306.16084. HPLC Rt = 1.33.

2-Methyl-5-phenyl-2H-pyrazole-3-carboxylic acid ((S)-1-phenyl-ethyl)-amide (12). The title compound was prepared according to General Method A from 2-methyl-5-phenyl-2H-pyrazole-3-carboxylic acid (25 mg, 0.12 mmol) in 31 mg (82%) yield. ^{1}H NMR (500 MHz, DMSO-d_6) δ 8.88 (br d, J=7.88 Hz, 1H), 7.77 (dd, J=1.26, 8.20 Hz, 2H), 7.44 (br s, 2H), 7.37-7.47 (m, 1H), 7.35-7.38 (m, 1H), 7.35-7.38 (m, 2H), 7.29-7.36 (m, 2H), 7.24 (t,

J=7.30 Hz, 1H), 5.13 (quin, J=7.25 Hz, 1H), 4.06 (s, 3H), 1.48 (d, J=6.94 Hz, 3H). ^{13}C NMR (125 MHz, DMSO-d_6) δ 158.5, 148.2, 144.5, 136.9, 132.6, 128.9, 128.4, 127.9, 126.8, 126.1, 125.0, 104.4, 48.2, 39.0, 22.2. HRMS (m/z): $[M+H]^+$ calcd. for $C_{19}H_{19}N_3O$, 306.16009; found, 306.16077. HPLC Rt = 1.33.

N-benzyl-1-methyl-3-phenyl-1H-pyrazole-5-carboxamide (13). The title compound was prepared according to General Method A from 2-methyl-5-phenyl-2H-pyrazole-3-carboxylic acid (70 mg, 0.35 mmol) in 67 mg (66%) yield. ^{1}H NMR (500 MHz, DMSO-d_6) δ 9.09 (br t, J=5.99 Hz, 1H), 7.75 (d, J=7.25 Hz, 2H), 7.43 (t, J=7.25 Hz, 2H), 7.29-7.37 (m, 6H), 7.25-7.28 (m, 1H), 4.47 (d, J=5.99 Hz, 2H), 4.11 (s, 3H). ^{13}C NMR (125 MHz, DMSO-d_6) δ 159.3, 148.2, 139.1, 136.8, 132.6, 128.9, 128.4, 127.8, 127.3, 126.9, 124.9, 104.2, 42.2, 39.0. HRMS (m/z): $[M+H]^+$ calcd. for $C_{18}H_{17}N_3O$, 292.14444; found, 292.14438. HPLC Rt = 1.27.

4-{2-[(1-methyl-3-phenyl-1H-pyrazol-5-yl)formamido]propan-2-yl}benzoic acid (14). The title compound was prepared according to General Method A and General Method B from 2-methyl-5-phenyl-2H-pyrazole-3-carboxylic acid (66 mg). ^{1}H NMR (400 MHz,

DMSO-d_6) δ 8.56-8.63 (m, 1H), 7.86 (d, J=8.36 Hz, 2H), 7.80 (d, J=7.35 Hz, 2H), 7.47 (d, J=7.35 Hz, 2H), 7.40-7.45 (m, 3H), 7.33 (t, J=7.35 Hz, 1H), 3.96 (s, 3H), 1.68 (s, 6H), acid OH not visible. ^{13}C NMR (100 MHz, DMSO-d_6) δ 168.0, 158.8, 151.3, 148.0, 137.3, 132.7, 131.6, 129.1, 128.8, 127.7, 124.9, 124.4, 104.6, 55.6, 38.9, 29.3. HRMS (m/z): $[M+H]^+$ calcd. for $C_{21}H_{21}N_3O_3$, 364.16557; found, 364.16591. HPLC Rt = 0.91.

4-[(1R)-1-[(1-methyl-3-phenyl-1H-pyrazol-5-yl)formamido]ethyl]benzoic acid (15). The title compound was prepared according to General Method A and General Method B from 2-methyl-5-phenyl-2H-pyrazole-3-carboxylic acid (138 mg). ^{1}H NMR (400 MHz, DMSO-d_6) δ 12.65-13.07 (m, 1H), 8.98 (d, J=7.86 Hz, 1H), 7.92 (d, J=8.11 Hz, 2H), 7.78 (d, J=7.35 Hz, 2H), 7.52 (d, J=8.11 Hz, 2H), 7.39-7.48 (m, 3H), 7.33 (t, J=7.35 Hz, 1H), 5.18 (quin, J=7.22 Hz, 1H), 4.06 (s, 3H), 1.50 (d, J=7.10 Hz, 3H). ^{13}C NMR (100 MHz, DMSO-d_6) δ 167.1, 158.6, 149.5, 148.1, 136.6, 132.6, 129.5, 129.3, 128.8, 127.8, 126.2, 124.9, 104.4, 48.1, 38.9, 21.9. HRMS (m/z): $[M+H]^+$ calcd. for $C_{20}H_{19}N_3O_3$, 350.14992; found, 350.15039. HPLC Rt = 0.85.

4-{[(1-methyl-3-phenyl-1H-pyrazol-5-yl)formamido]methyl}benzoic acid (16). The title compound was prepared according to General Method A and General Method B from 2-methyl-5-phenyl-2H-pyrazole-3-carboxylic acid (8 mg). ^{1}H NMR (500 MHz, DMSO-d_6) δ 12.73 (s, 1H), 9.18 (t, J=5.99 Hz, 1H), 7.92 (d, J=8.51 Hz, 2H), 7.76 (dd, J=1.10, 8.35 Hz, 2H), 7.38-7.48 (m, 4H), 7.28-7.36 (m, 2H), 4.53 (d, J=5.99 Hz, 2H), 4.11 (s, 3H). ^{13}C NMR (125 MHz, DMSO-d_6) δ 167.2, 159.4, 148.3, 144.3, 136.6, 132.5, 129.5, 129.4, 128.9, 127.9, 127.3, 124.9, 104.2, 42.0, 39.1. HRMS (m/z): $[M+H]^+$ calcd. for $C_{19}H_{17}N_3O_3$, 336.13427; found, 336.13482. HPLC Rt = 0.78.

4-{1-[(1-methyl-3-phenyl-1H-pyrazol-5-yl)formamido]ethyl}benzoic acid (17). The title compound was prepared according to General Method A and General Method B from 2-methyl-5-phenyl-2H-pyrazole-3-carboxylic acid (14 mg). ^{1}H NMR (500 MHz, DMSO-d_6) δ 12.07-13.55 (m, 1H), 8.96 (d, J=7.88 Hz, 1H), 7.92 (d, J=8.20 Hz, 2H), 7.78 (d, J=7.88 Hz, 2H), 7.51 (d, J=8.20 Hz, 2H), 7.39-7.47 (m, 3H), 7.33 (t, J=7.88 Hz, 1H), 5.10-5.30 (m, 1H), 4.05 (s, 3H), 1.49 (s, 3H). ^{13}C NMR (125 MHz, DMSO-d_6) δ 167.2, 158.6, 149.5, 148.2, 136.7, 132.6, 129.5, 129.3, 128.9, 127.8, 126.2, 124.9, 104.4, 48.2, 39.0,

21.9. HRMS (m/z): $[M+H]^+$ calcd. for $C_{20}H_{19}N_3O_3$, 350.14992; found, 350.15028. HPLC Rt = 0.86.

1-Methyl-3-phenyl-N-[1-(4-sulfamoylphenyl)ethyl]-1H-pyrazole-5-carboxamide (18). The title compound was prepared according to General Method A from 2-methyl-5-phenyl-2H-pyrazole-3-carboxylic acid (55 mg, 0.27 mmol) in 105 mg (82%) yield. ^{1}H NMR (500 MHz, DMSO-d_6) δ 9.00 (d, J=7.57 Hz, 1H), 7.74-7.82 (m, 4H), 7.58 (d, J=8.20 Hz, 2H), 7.41-7.47 (m, 3H), 7.28-7.36 (m, 3H), 5.16 (quin, J=7.17 Hz, 1H), 4.05 (s, 3H), 1.50 (d, J=7.25 Hz, 3H). ^{13}C NMR (125 MHz, DMSO-d_6) δ 158.6, 148.6, 148.1, 142.6, 136.6, 132.6, 128.9, 127.8, 126.5, 125.8, 124.9, 104.5, 48.2, 39.0, 22.0. HRMS (m/z): $[M+H]^+$ calcd. for $C_{19}H_{20}N_4O_3S$, 385.13289; found, 385.13405. HPLC Rt = 1.08.

2-Methyl-5-phenyl-2H-pyrazole-3-carboxylic acid [(R)-1-(4-nitro-phenyl)-ethyl]-amide (19). The title compound was prepared according to General Method A from 2-methyl-5-phenyl-2H-pyrazole-3-carboxylic acid (1.00 g, 4.87 mmol) in 1.60 g (94%) yield. ^{1}H NMR (500 MHz, DMSO-d_6) δ 9.04 (d, J=7.57 Hz, 1H), 8.23 (d, J=8.70 Hz, 2H), 7.79 (d,

J=7.25 Hz, 2H), 7.68 (d, J=8.70 Hz, 2H), 7.42-7.48 (m, 3H), 7.34 (t, J=7.30 Hz, 1H), 5.23 (quin, J=7.17 Hz, 1H), 4.06 (s, 3H), 1.52 (d, J=6.94 Hz, 3H). ^{13}C NMR (125 MHz, DMSO-d_6) δ 158.7, 152.4, 148.1, 146.4, 136.5, 132.5, 128.8, 127.8, 127.3, 124.9, 123.6, 104.5, 48.2, 39.4, 21.8. HRMS (m/z): $[M+H]^+$ calcd. for $C_{19}H_{18}N_4O_3$, 351.14517; found, 351.14532. HPLC Rt = 1.41.

2-Methyl-5-phenyl-2H-pyrazole-3-carboxylic acid [(R)-1-(4-amino-phenyl)-ethyl]-amide (20). 2-Methyl-5-phenyl-2H-pyrazole-3-carboxylic acid [(R)-1-(4-nitro-phenyl)-ethyl]-amide (**19**) (600 mg, 1.71 mmol), 10% Pd/C (91 mg, 0.09 mmol), and ammonium formate (756 mg, 12 mmol) in MeOH (6 mL) were stirred at room temperature for 2 h. The mixture was filtered and concentrated in vacuo. The residue was partitioned between water and CH_2Cl_2, and the organic layer was washed with water and saturated aqueous NaCl solution. The organic layer was dried (Na_2SO_4) and concentrated in vacuo to give **20** in 480 mg (87%) yield. ^{1}H NMR (500 MHz, DMSO-d_6) δ 8.65 (d, J=8.51 Hz, 1H), 7.77 (d, J=7.30 Hz, 2H), 7.43 (t, J=7.30 Hz, 2H), 7.36 (s, 1H), 7.32 (t, J=7.30 Hz, 1H), 7.05 (d, J=8.50 Hz, 2H), 6.53 (d, J=8.51 Hz, 2H), 4.89-5.26 (m, 3H),

4.08 (s, 3H), 1.42 (q, J=6.94 Hz, 3H). ^{13}C NMR (125 MHz, DMSO-d_6) δ 158.2, 148.0, 147.5, 137.0, 132.6, 131.1, 128.8, 127.7, 126.8, 124.9, 113.6, 104.1, 47.4, 39.4, 22.0. HRMS (m/z): $[M+H]^+$ calcd. for $C_{19}H_{20}N_4O$, 321.17099; found, 321.17099. HPLC Rt = 1.21.

N-[(1R)-1-(4-iodophenyl)ethyl]-1-methyl-3-phenyl-1H-pyrazole-5-carboxamide (Int-02). The title compound was prepared according to General Method A from 2-methyl-5-phenyl-2H-pyrazole-3-carboxylic acid (1.58 g, 7.70 mmol) in 2.66 g (80%) yield. ^{1}H NMR (500 MHz, DMSO-d_6) δ 8.90 (br d, J=7.88 Hz, 1H), 7.78 (d, J=7.88 Hz, 2H), 7.71 (d, J=8.20 Hz, 2H), 7.44 (t, J=7.80 Hz, 2H), 7.39 (s, 1H), 7.33 (t, J=7.80 Hz, 1H), 7.22 (d, J=8.20 Hz, 2H), 5.08 (quin, J=7.17 Hz, 1H), 4.06 (s, 3H), 1.46 (d, J=6.94 Hz, 3H). ^{13}C NMR (126 MHz, DMSO-d_6) δ 158.6, 148.2, 144.4, 137.1, 136.7, 132.6, 128.9, 128.6, 127.8, 124.9, 104.4, 92.5, 47.9, 21.9, 1 C under DMSO signal. HRMS (m/z): $[M+H]^+$ calcd. for $C_{19}H_{18}IN_3O$, 432.05674, found, 432.05716. HPLC Rt = 1.48.

2-Methyl-5-phenyl-2H-pyrazole-3-carboxylic acid {(R)-1-[4-(2-oxo-pyrrolidin-1-yl)-phenyl]-ethyl}-amide (21). **General Method C**. N-[(1R)-1-(4-iodophenyl)ethyl]-1-methyl-

3-phenyl-1H-pyrazole-5-carboxamide (**Int-02**) (80 mg, 0.19 mmol), 2-pyrrolidone (12 µL, 0.15 mmol), K_2CO_3 (52 mg, 0.37 mmol), N,N'-dimethylethylenediamine (20 µL, 0.19 mmol), and CuI (11mg, 0.06 mmol) in dr DMF (500 µL) were stirred for 48 h at 90 °C. The mixture was filtered and concentrated in vacuo, and the crude product was purified by prep. HPLC (MeCN/water) to give **21** in 32 mg (44%) yield. ^{1}H NMR (500 MHz, DMSO-d_6) δ 8.86 (d, J=7.88 Hz, 1H), 7.77 (d, J=7.50 Hz, 2H), 7.59 (d, J=8.83 Hz, 2H), 7.43 (t, J=7.50 Hz, 2H), 7.36-7.41 (m, 3H), 7.32 (t, J=7.50 Hz, 1H), 5.11 (quin, J=7.17 Hz, 1H), 4.06 (s, 3H), 3.81 (t, J=7.50 Hz, 2H), 2.47 (t, J=7.90 Hz, 2H), 2.05 (quin, J=7.57 Hz, 2H), 1.47 (d, J=6.94 Hz, 3H). ^{13}C NMR (125 MHz, DMSO-d_6) δ 173.7, 158.5, 148.1, 139.9, 138.3, 136.8, 132.6, 128.9, 127.8, 126.3, 124.9, 119.5, 104.3, 48.1, 47.8, 39.0, 32.3, 22.1, 17.5. HRMS (m/z): $[M+H]^+$ calcd. for $C_{23}H_{24}N_4O_2$, 389.19720; found, 389.19693. HPLC Rt = 1.20.

N-[1-(4-methanesulfonylphenyl)ethyl]-1-methyl-3-phenyl-1H-pyrazole-5-carboxamide (22). The title compound was prepared according to General Method A from 2-methyl-5-phenyl-2H-pyrazole-3-carboxylic acid (50 mg, 0.24 mmol) in 24 mg (26%) yield. ^{1}H NMR

(500 MHz, DMSO-d_6) δ 9.01 (d, J=7.57 Hz, 1H), 7.90 (d, J=8.30 Hz, 2H), 7.78 (d, J=7.25 Hz, 2H), 7.66 (d, J=8.30 Hz, 2H), 7.39-7.48 (m, 3H), 7.33 (t, J=7.25 Hz, 1H), 5.20 (quin, J=7.17 Hz, 1H), 4.05 (s, 3H), 3.20 (s, 3H), 1.51 (d, J=6.94 Hz, 3H). ^{13}C NMR (125 MHz, DMSO-d_6) δ 158.7, 150.6, 148.2, 139.3, 136.6, 132.6, 128.9, 127.9, 127.2, 127.0, 124.9, 104.5, 48.3, 43.6, 39.0, 22.0. HRMS (m/z): $[M+H]^+$ calcd. for $C_{20}H_{21}N_3O_3S$, 384.13764; found, 384.13841. HPLC Rt = 1.18.

N-[(1R)-1-(4-bromophenyl)ethyl]-1-methyl-3-phenyl-1H-pyrazole-5-carboxamide (**Int-03**). The title compound was prepared according to General Method A from 2-methyl-5-phenyl-2H-pyrazole-3-carboxylic acid (400 mg, 1.95 mmol) in 658 mg (88%) yield and used in the next steps without further purification.

N-[(1R)-1-{4-[(3R,4S)-3,4-dihydroxypyrrolidin-1-yl]phenyl}ethyl]-1-methyl-3-phenyl-1H-pyrazole-5-carboxamide (23). **General Method D**. To N-[(1R)-1-(4-bromophenyl)ethyl]-1-methyl-3-phenyl-1H-pyrazole-5-carboxamide (**Int-03**) (50 mg, 0.13 mmol), sodium tert.-butoxide (50 mg, 0.52 mmol), 2-(di-tert.-butylphosphino)biphenyl (16 mg, 0.05 mmol), and tris(dibenzylideneacetone)dipalladium(0) (12 mg, 0.01 mmol) in dry dioxane (3 mL)

cis-pyrrolidine-3,4-diol hydrochloride (27 mg, 0.20 mmol) was added under argon and stirred for 16 h at 50 °C. The mixture was filtered and concentrated in vacuo, and the crude product was purified by prep. HPLC (MeCN/water) to give **23** in 12 mg (23%) yield. ^{1}H NMR (500 MHz, DMSO-d_6) δ 8.69 (d, J=8.20 Hz, 1H), 7.76 (d, J=7.70 Hz, 2H), 7.43 (br t, J=7.70 Hz, 2H), 7.35 (s, 1H), 7.32 (t, J=7.70 Hz, 1H), 7.18 (d, J=8.51 Hz, 2H), 6.43 (d, J=8.83 Hz, 2H), 5.03 (quin, J=7.25 Hz, 1H), 4.87 (d, J=4.41 Hz, 2H), 4.08-4.15 (m, 2H), 4.06 (s, 3H), 3.00-3.11 (m, 2H), 1.43 (d, J=6.94 Hz, 3H), OH protons not visible. ^{13}C NMR (125 MHz, DMSO-d_6) δ 158.2, 148.1, 146.7, 137.0, 132.6, 130.7, 128.8, 127.8, 127.0, 124.9, 110.8, 104.2, 70.6, 52.5, 47.5, 39.0, 22.1. HRMS (m/z): $[M+H]^+$ calcd. for $C_{23}H_{26}N_4O_3$, 407.20777; found, 407.20825. HPLC Rt = 1.13.

N-[(1R)-1-{4-[(3S)-3-hydroxypyrrolidin-1-yl]phenyl}ethyl]-1-methyl-3-phenyl-1H-pyrazole-5-carboxamide (24). The title compound was prepared according to General Method D from **Int-03** (200 mg, 0.52 mmol) in 130 mg (64%) yield. ^{1}H NMR (500 MHz, DMSO-d_6) δ 8.69 (d, J=8.20 Hz, 1H), 7.76 (d, J=7.25 Hz, 2H), 7.43 (t, J=7.72 Hz, 2H), 7.35 (s, 1H), 7.32 (t, J=7.70 Hz, 1H), 7.19 (d, J=8.51 Hz, 2H), 6.47 (d, J=8.51 Hz, 2H),

5.04 (quin, J=7.25 Hz, 1H), 4.33-4.42 (m, 1H), 4.06 (s, 3H), 3.15-3.31 (m, 2H), 3.03 (dd, J=1.58, 10.09 Hz, 1H), 1.96-2.07 (m, 1H), 1.82-1.91 (m, 1H), 1.44 (d, J=7.25 Hz, 3H), 1 H under H_2O signal, COOH not visible. ^{13}C NMR (125 MHz, DMSO-d_6) δ 158.2, 148.1, 146.8, 137.0, 132.6, 130.7, 128.8, 127.8, 126.9, 124.9, 111.2, 104.2, 69.3, 56.1, 47.5, 45.6, 39.0, 33.8, 22.1. HRMS (m/z): $[M+H]^+$ calcd. for $C_{23}H_{26}N_4O_2$, 391.21285; found, 391.21347. HPLC Rt = 1.22.

1-Methyl-3-phenyl-N-[(1R)-1-[4-(pyrrolidin-1-yl)phenyl]ethyl]-1H-pyrazole-5-carboxamide (25). The title compound was prepared according to General Method D from **Int-03** (200 mg, 0.52 mmol) in 120 mg (62%) yield. ^1H NMR (500 MHz, DMSO-d_6) δ 8.69 (d, J=8.20 Hz, 1H), 7.76 (d, J=7.88 Hz, 2H), 7.43 (br t, J=7.88 Hz, 2H), 7.36 (s, 1H), 7.32 (t, J=7.30 Hz, 1H), 7.19 (d, J=8.51 Hz, 2H), 6.50 (d, J=8.51 Hz, 2H), 5.04 (quin, J=7.25 Hz, 1H), 4.07 (s, 3H), 3.12-3.24 (m, 4H), 1.87-2.02 (m, 4H), 1.44 (d, J=6.94 Hz, 3H). ^{13}C NMR (125 MHz, DMSO-d_6) δ 158.2, 148.0, 146.8, 137.0, 132.6, 130.7, 128.8, 127.7, 126.9, 124.9, 111.4, 104.1, 47.5, 47.4, 24.9, 22.1, 1 C under

DMSO signal. HRMS (m/z): $[M+H]^+$ calcd. $C_{23}H_{26}N_4O$, 375.21794; found, 375.21823. HPLC Rt = 1.52.

N-{1-[4-(1,1-dioxo-1λ⁶,2-thiazolidin-2-yl)phenyl]ethyl}-1-methyl-3-phenyl-1H-pyrazole-5-carboxamide (Int-04). The title compound was prepared according to General Method A from 2-methyl-5-phenyl-2H-pyrazole-3-carboxylic acid (350 mg, 1.64 mmol) in 643 mg (92%) yield. ^{1}H NMR (400 MHz, DMSO-d_6) δ 8.86 (br d, J=7.86 Hz, 1H), 7.77 (br d, J=7.35 Hz, 2H), 7.36-7.48 (m, 5H), 7.33 (br t, J=7.60 Hz, 1H), 7.18 (br d, J=7.35 Hz, 2H), 5.11 (br t, J=6.84 Hz, 1H), 4.06 (br s, 3H), 3.72 (br s, 2H), 3.49 (br t, J=7.22 Hz, 2H), 2.39 (br t, J=6.59 Hz, 2H), 1.47 (br d, J=6.34 Hz, 3H). ^{13}C NMR (100 MHz, DMSO-d_6) δ 158.5, 148.1, 139.7, 136.8, 132.6, 128.8, 127.8, 127.0, 124.9, 118.6, 104.3, 48.2, 47.7, 46.6, 38.9, 22.1, 18.5. HRMS (m/z): $[M+H]^+$ calcd. for $C_{22}H_{24}N_4O_3S$, 425.16419; found, 425.16431. HPLC Rt = 1.21.

Chiral separation of this material **yielded (R)-N-{1-[4-(1,1-dioxo-1λ⁶,2-thiazolidin-2-yl)phenyl]ethyl}-1-methyl-3-phenyl-1H-pyrazole-5-carboxamide (26)** in 30 mg (38%) yield. ^{1}H NMR (500 MHz, DMSO-d_6) δ 8.86 (br d, J=8.20 Hz, 1H), 7.78 (d, J=7.57 Hz,

2H), 7.38-7.47 (m, 5H), 7.33 (t, J=7.20 Hz, 1H), 7.19 (d, J=8.51 Hz, 2H), 5.12 (quin, J=7.17 Hz, 1H), 4.07 (s, 3H), 3.73 (t, J=6.46 Hz, 2H), 3.50 (t, J=7.41 Hz, 2H), 2.40 (td, J=6.98, 14.11 Hz, 2H), 1.48 (d, J=6.94 Hz, 3H). ^{13}C NMR (125 MHz, DMSO-d_6) δ 158.4, 148.1, 139.6, 136.8, 132.6, 128.8, 127.8, 126.9, 124.9, 118.5, 104.3, 48.1, 47.6, 46.6, 39.4, 22.0, 18.5 , 1 carbon under DMSO signal. HRMS (m/z): $[M+H]^+$ calcd. for $C_{22}H_{24}N_4O_3S$, 425.16419; found, 425.16432. HPLC Rt = 1.29.

N-[(1R)-1-[4-(2,5-dioxoimidazolidin-1-yl)phenyl]ethyl]-1-methyl-3-phenyl-1H-pyrazole-5-carboxamide (27).To 2-methyl-5-phenyl-2H-pyrazole-3-carboxylic acid [(R)-1-(4-amino-phenyl)-ethyl]-amide (**20**) (50 mg, 0.16 mmol) and triethyl amine (32 µL, 0.23 mmol) in dry DMF (500 µL) ethyl isocyanate (30 mg, 0.23 mmol) was added and stirred for 16 h at room temperature. Then sodium ethoxide (21% in EtOH, 29 µL, 0.078 mmol) was added and stirred for additional 2 h. The mixture was filtered and concentrated in vacuo, and the crude product was purified by prep. HPLC (MeCN/water) to give **27** in 11 mg (17%) yield. ^{1}H NMR (500 MHz, DMSO-d_6) δ 8.93 (d, J=7.88 Hz, 1H), 8.28 (s, 1H), 7.78 (d, J=7.57 Hz, 2H), 7.49 (d, J=8.20 Hz, 2H), 7.40-7.46 (m, 2H), 7.39 (br s, 1H),

7.27-7.35 (m, 3H), 5.16 (quin, J=7.09 Hz, 1H), 4.00-4.13 (m, 5H), 1.51 (d, J=7.25 Hz, 3H). ^{13}C NMR (125 MHz, DMSO-d_6) δ 171.1, 158.5, 156.5, 148.1, 144.0, 136.7, 132.6, 130.8, 128.8, 127.8, 126.7, 126.4, 124.9, 104.4, 47.9, 46.0, 39.0, 22.1. HRMS (m/z): $[M+H]^+$ calcd. for $C_{22}H_{21}N_5O_3$, 404.17172; found, 404.17183. HPLC Rt = 1.08.

(2S)-1-{4-[(1R)-1-[(1-methyl-3-phenyl-1H-pyrazol-5-yl)formamido]ethyl]phenyl}-5-oxopyrrolidine-2-carboxylic acid (28). (S)-1-(4-{(R)-1-[(2-Methyl-5-phenyl-2H-pyrazole-3-carbonyl)-amino]-ethyl}-phenyl)-5-oxo-pyrrolidine-2-carboxylic acid ethyl ester was prepared from N-[(1R)-1-(4-iodophenyl)ethyl]-1-methyl-3-phenyl-1H-pyrazole-5-carboxamide (**Int-02**) (200 mg, 0.46 mmol) according to General Method C in 40 mg (19%) yield. The crude material (28 mg, 0.06 mmol) was saponified according to General Method B to give (2S)-1-{4-[(1R)-1-[(1-methyl-3-phenyl-1H-pyrazol-5-yl)formamido]ethyl]phenyl}-5-oxopyrrolidine-2-carboxylic acid (**28**) in 20 mg (76%) yield. ^{1}H NMR (400 MHz, DMSO-d_6) δ 13.01-13.31 (m, 1H), 8.86 (d, J=7.86 Hz, 1H), 7.78 (d, J=8.00 Hz, 2H), 7.37-7.50 (m, 7H), 7.33 (t, J=7.00 Hz, 1H), 5.12 (quin, J=7.22 Hz, 1H), 4.76-4.89 (m, 1H), 4.06 (s, 3H), 2.00-2.13 (m, 1H), 1.47 (d, J=7.10 Hz, 3H), 3Hs under

DMSO signal. ^{13}C NMR (100 MHz, DMSO-d_6) δ 173.3, 172.7, 157.8, 147.5, 139.9, 136.7, 136.2, 132.0, 128.2, 127.1, 125.8, 124.3, 120.1, 103.7, 60.0, 47.0, 30.0, 21.9, 21.4 , 1 C under DMSO signal. HRMS (m/z): $[M+H]^+$ calcd. for $C_{24}H_{24}N_4O_4$, 433.18703; found, 433.18706. HPLC Rt = 0.84.

2-Methyl-5-phenyl-2H-pyrazole-3-carboxylic acid [(R)-1-(4-guanidino-phenyl)-ethyl]-amide (29). 2-Methyl-5-phenyl-2H-pyrazole-3-carboxylic acid [(R)-1-(4-amino-phenyl)-ethyl]-amide **(20**) (50 mg, 0.16 mmol) and cyanamide (8 mg, 0.19 mmol) in dioxane (500 µL) were treated with 4 N HCl in dioxane (58 µL) and stirred for 1 h at 120 °C in a microwave reactor. The mixture was concentrated in vacuo, and the crude product was purified by prep. HPLC (MeCN/water) to give **29** in 12 mg (21%) yield. ^{1}H NMR (500 MHz, DMSO-d_6) δ 8.91 (d, J=7.88 Hz, 1H), 7.81-8.07 (m, 4H), 7.78 (d, J=7.25 Hz, 2H), 7.37-7.48 (m, 5H), 7.33 (t, J=7.30 Hz, 1H), 7.16 (d, J=8.51 Hz, 2H), 5.14 (quin, J=7.25 Hz, 1H), 4.06 (s, 3H), 1.48 (d, J=6.94 Hz, 3H). ^{13}C NMR (125 MHz, DMSO-d_6) δ 167.7, 158.4, 156.1, 148.1, 141.8, 136.8, 132.6, 128.9, 127.8, 127.2, 124.9, 123.8, 104.3, 47.8,

39.0, 22.2. HRMS (m/z): $[M+H]^+$ calcd. for $C_{20}H_{22}N_6O$, 363.19279; found, 363.19270. HPLC Rt = 0.95.

1-Methyl-N-{1-[4-(1-methylcarbamimidamido)phenyl]ethyl}-3-phenyl-1H-pyrazole-5-carboxamide (30). 1-Methyl-4-phenyl-1H-pyrazole-3-carboxylic acid (3.00 g, 14.9 mmol) and [4-(1-amino-ethyl)-phenyl]-methyl-carbamic acid tert-butyl ester (4.46 g, 17.8 mmol) were reacted according to General Method A to give methyl-(4-{1-[(2-methyl-5-phenyl-2H-pyrazole-3-carbonyl)-amino]-ethyl}-phenyl)-carbamic acid tert-butyl ester in 2.60 g (40%) yield. The crude material (2.00 g, 4.61 mmol) in dry dioxane (20 mL) was treated with HCl (4 N in dioxane, 20 mL) to give 2-methyl-5-phenyl-2H-pyrazole-3-carboxylic acid [1-(4-methylamino-phenyl)-ethyl]-amide hydrochloride in a quantitative yield upon evaporation. The crude material was reacted with cyanamide as described for the synthesis of **29** to give the target compound **30** in 76 mg (14%) yield. ^{1}H NMR (500 MHz, DMSO-d_6) δ 8.88 (s, 1H), 7.78 (d, J=7.25 Hz, 2H), 7.38-7.48 (m, 5H), 7.33 (t, J=7.30 Hz, 1H), 7.26 (d, J=8.20 Hz, 2H), 5.17 (q, J=6.94 Hz, 1H), 4.07 (s, 3H), 3.17 (s, 3H), 1.49 (d, J=7.25 Hz, 3H), NH_2 and NH not visible. ^{13}C NMR (125 MHz, DMSO-d_6) δ

159.1, 158.4, 148.1, 142.7, 142.0, 136.7, 132.6, 128.9, 127.8, 127.3, 126.3, 124.9, 104.3, 47.7, 38.9, 22.2, 1 C under DMSO signal. HRMS (m/z): $[M+H]^+$ calcd. for $C_{21}H_{24}N_6O$, 377.20844; found, 377.20804. HPLC Rt = 1.12.

1-Methyl-N-{1-[4-(N-methylmethanesulfonamido)phenyl]ethyl}-3-phenyl-1H-pyrazole-5-carboxamide (31). Crude 2-methyl-5-phenyl-2H-pyrazole-3-carboxylic acid [1-(4-methylamino-phenyl)-ethyl]-amide hydrochloride (200 mg, 0.60 mmol) from the above synthesis in dry CH_2Cl_2 (2 mL) was treated with methane sulfonyl chloride (200 µL, 1.21 mmol) and triethyl amine (120 µL, 0.91 mmol) and stirred for 12 h at room temperature. The mixture was concentrated in vacuo, and the crude product was purified by prep. HPLC (MeCN/water) to give **31** in 165 mg (67%) yield. ^{1}H NMR (400 MHz, DMSO-d_6) δ 8.91 (d, J=7.86 Hz, 1H), 7.78 (d, J=7.20 Hz, 2H), 7.39-7.47 (m, 5H), 7.34-7.39 (m, 2H), 7.29-7.35 (m, 1H), 5.15 (quin, J=7.22 Hz, 1H), 4.06 (s, 3H), 3.21 (s, 3H), 2.93 (s, 3H), 1.48 (d, J=6.84 Hz, 3H). ^{13}C NMR (100 MHz, DMSO-d_6) δ 158.5, 148.2, 143.3, 140.3, 136.7, 132.6, 128.9, 127.8, 126.8, 126.4, 124.9, 104.4, 47.8, 38.9, 37.9, 35.0, 22.1.

HRMS (m/z): $[M+H]^+$ calcd. for $C_{21}H_{24}N_4O_3S$, 413.16419; found, 413.16382. HPLC Rt = 1.29.

2-Methyl-5-phenyl-2H-pyrazole-3-carboxylic acid [(R)-1-(4-methanesulfonylamino-phenyl)-ethyl]-amide (32). 2-Methyl-5-phenyl-2H-pyrazole-3-carboxylic acid [(R)-1-(4-amino-phenyl)-ethyl]-amide (**20**) (50 mg, 0.16 mmol) and Et_3N (25 µL, 0.17 mmol) in dry CH_2Cl_2 (0.5 mL) were treated with methanesulfonyl chloride (13 µL, 0.17 mmol) and stirred at room temperature overnight. The mixture was concentrated in vacuo. The crude product was purified by prep. HPLC (MeCN/water) to give **32** in 24 mg (39%) yield. ^{1}H NMR (500 MHz, DMSO-d_6) δ 9.68 (s, 1H), 8.84 (d, J=7.88 Hz, 1H), 7.78 (d, J=7.25 Hz, 2H), 7.44 (t, J=7.25 Hz, 2H), 7.40 (s, 1H), 7.37 (d, J=8.51 Hz, 2H), 7.33 (t, J=7.25 Hz, 1H), 7.18 (d, J=8.51 Hz, 2H), 5.11 (quin, J=7.17 Hz, 1H), 4.07 (s, 3H), 2.97 (s, 3H), 1.47 (d, J=6.94 Hz, 3H). ^{13}C NMR (125 MHz, DMSO-d_6) δ 158.4, 148.1, 139.9, 137.0, 136.8, 132.6, 128.8, 127.8, 127.0, 124.9, 120.0, 104.3, 47.6, 22.0, 2 Cs under DMSO signal. HRMS (m/z): $[M+H]^+$ calcd. for $C_{20}H_{22}N_4O_3S$, 399.14854; found, 399.14872. HPLC Rt = 1.22.

N-[(1R)-1-(4-Methoxyphenyl)ethyl]-1-methyl-3-phenyl-1H-pyrazole-5-carboxamide (33). The title compound was prepared according to General Method A from 2-methyl-5-phenyl-2H-pyrazole-3-carboxylic acid (50 mg, 0.24 mmol) in 13 mg (16%) yield. ^{1}H NMR (500 MHz, DMSO-d_6) δ 8.79 (br d, J=8.20 Hz, 1H), 7.77 (d, J=8.20 Hz, 2H), 7.43 (t, J=7.70 Hz, 2H), 7.37 (s, 1H), 7.29-7.35 (m, 3H), 6.90 (d, J=8.20 Hz, 2H), 5.10 (quin, J=7.25 Hz, 1H), 4.06 (s, 3H), 3.73 (s, 3H), 1.46 (d, J=6.94 Hz, 3H). ^{13}C NMR (125 MHz, DMSO-d_6) δ 158.3, 158.1, 148.1, 136.9, 136.3, 132.6, 128.8, 127.8, 127.3, 124.9, 113.7, 104.2, 55.1, 47.5, 39.0, 22.1. HRMS (m/z): $[M+H]^+$ calcd. for $C_{20}H_{21}N_3O_2$, 336.17065; found, 336.17096. HPLC Rt = 1.32.

N-[(1R)-1-(4-carbamoylphenyl)ethyl]-1-methyl-3-phenyl-1H-pyrazole-5-carboxamide (34). 4-[(1R)-1-[(1-methyl-3-phenyl-1H-pyrazol-5-yl)formamido]ethyl]benzoic acid (**15**) (86 mg, 0.24 mmol) in dry CH_2Cl_2 (3 mL) was treated with cat. DMF and oxalyl chloride (31 µL, 0.36 mmol). The mixture was stirred for 30 min at room temperature, then ammonia (7 N in MeOH, 200 µL) was added and stirred for 1 h. The mixture was concentrated in vacuo. The crude product was purified by prep. HPLC (MeCN/water) to

give **34** in 50 mg (59%) yield. ^{1}H NMR (500 MHz, DMSO-d_6) δ 8.93 (d, J=7.88 Hz, 1H), 7.93 (br s, 1H), 7.83 (d, J=8.20 Hz, 2H), 7.78 (d, J=7.25 Hz, 2H), 7.36-7.49 (m, 5H), 7.33 (s, 2H), 5.16 (quin, J=7.25 Hz, 1H), 4.05 (s, 3H), 1.49 (d, J=7.25 Hz, 3H). ^{13}C NMR (125 MHz, DMSO-d_6) δ 167.8, 158.6, 148.2, 147.8, 136.8, 132.9, 132.6, 128.9, 127.9, 127.7, 125.9, 125.0, 104.4, 48.1, 39.0, 22.1. HRMS (m/z): $[M+H]^+$ calcd. for $C_{20}H_{20}N_4O_2$, 349.16590; found, 349.16635. HPLC Rt = 1.06.

1-Methyl-3-phenyl-N-{1-[4-(pyrimidin-5-yl)phenyl]ethyl}-1H-pyrazole-5-carboxamide (35). The title compound was prepared according to General Method A from 2-methyl-5-phenyl-2H-pyrazole-3-carboxylic acid (25 mg, 0.12 mmol) in 20 mg (74%) yield. ^{1}H NMR (400 MHz, DMSO-d_6) δ 9.18 (s, 1H), 9.13 (s, 2H), 8.96 (d, J=7.86 Hz, 1H), 7.75-7.82 (m, 4H), 7.56 (d, J=8.11 Hz, 2H), 7.39-7.48 (m, 3H), 7.33 (t, J=7.30 Hz, 1H), 5.19 (quin, J=7.22 Hz, 1H), 4.06 (s, 3H), 1.52 (d, J=7.10 Hz, 3H). ^{13}C NMR (100 MHz, DMSO-d_6) δ 158.6, 157.2, 154.7, 148.2, 145.4, 136.8, 133.1, 132.6, 132.3, 128.9, 127.9, 127.0, 124.9, 104.4, 48.1, 39.6, 22.1. HRMS (m/z): $[M+H]^+$ calcd. for $C_{23}H_{21}N_5O$, 384.18189; found, 384.18155. HPLC Rt = 1.20.

1-Methyl-N-[(1R)-1-(4-methylphenyl)ethyl]-3-phenyl-1H-pyrazole-5-carboxamide (36).

The title compound was prepared according to General Method A from 2-methyl-5-phenyl-2H-pyrazole-3-carboxylic acid (30 mg, 0.15 mmol) in 82 mg (82%) yield. 1H NMR (400 MHz, DMSO-d6) δ 8.82 (d, J=8.11 Hz, 1H), 7.77 (d, J=7.80 Hz, 2H), 7.43 (t, J=7.50 Hz, 2H), 7.39 (s, 1H), 7.32 (t, J=7.50 Hz, 1H), 7.28 (d, J=7.90 Hz, 2H), 7.14 (d, J=7.90 Hz, 2H), 5.10 (quin, J=7.22 Hz, 1H), 4.06 (s, 3H), 2.27 (s, 3H), 1.46 (d, J=7.10 Hz, 3H). 13C NMR (100 MHz, DMSO-d6) δ 158.4, 148.1, 141.4, 136.9, 135.8, 128.8, 127.8, 126.0, 124.9, 104.3, 47.8, 38.9, 22.2, 20.6 . HRMS (m/z): [M+H]+ calcd. for C20H21N3O, 320.17574; found, 320.17691. HPLC Rt = 1.40.

N-[(1R)-1-[4-(hydroxymethyl)phenyl]ethyl]-1-methyl-3-phenyl-1H-pyrazole-5-carboxamide (37). To methyl 4-[(1R)-1-[(1-methyl-3-phenyl-1H-pyrazol-5-yl)formamido]ethyl]benzoate (prepared according to General Method A, 300 mg, 0.83 mmol) in dry THF (10 mL) lithium aluminum hydride (1 M in THF, 3 mL, 3 mmol) was added at 0 °C. The mixture was stirred for 16 h at room temperature, quenched with water and filtered. The filtrate was concentrated in vacuo, and the crude product was

purified by prep. HPLC (MeCN/water) to give 37 in 140 mg (51%) yield. 1H NMR (500 MHz, DMSO-d6) δ 8.84 (br d, J=8.20 Hz, 1H), 7.78 (br d, J=7.25 Hz, 2H), 7.43 (t, J=7.57 Hz, 2H), 7.40 (s, 1H), 7.30-7.37 (m, 3H), 7.28 (br d, J=7.88 Hz, 2H), 5.07-5.19 (m, 1H), 4.46 (d, J=5.67 Hz, 2H), 4.06 (s, 3H), 1.47 (d, J=6.94 Hz, 3H) OH under signal at 5.12ppm. 13C NMR (125 MHz, DMSO-d6) δ 158.4, 148.1, 142.8, 141.0, 136.8, 132.6, 128.8, 127.8, 126.5, 125.8, 124.9, 104.3, 62.7, 48.0, 22.2, 1 C under DMSO signal. HRMS (m/z): [M+H]+ calcd. for C20H21N3O2, 336.17065; found, 336.17119. HPLC Rt = 1.13.

N-[1-(4-Cyanophenyl)ethyl]-1-methyl-3-phenyl-1H-pyrazole-5-carboxamide (38). The title compound was prepared according to General Method A from 2-methyl-5-phenyl-2H-pyrazole-3-carboxylic acid (25 mg, 0.12 mmol) in 18 mg (75%) yield. 1H NMR (500 MHz, DMSO-d6) δ 8.98 (d, J=7.57 Hz, 1H), 7.82 (d, J=8.20 Hz, 2H), 7.78 (d, J=6.94 Hz, 2H), 7.60 (d, J=8.51 Hz, 2H), 7.42-7.47 (m, 2H), 7.42 (s, 1H), 7.33 (t, J=7.60 Hz, 1H), 5.18 (quin, J=7.25 Hz, 1H), 4.05 (s, 3H), 1.49 (d, J=6.94 Hz, 3H). 13C NMR (126 MHz, DMSO-d6) δ 158.6, 150.3, 148.1, 136.5, 132.5, 132.4, 128.8, 127.8, 127.1, 124.9,

118.9, 109.6, 104.4, 48.2, 21.8, 1 C under DMSO signal. HRMS (m/z): [M+H]+ calcd. for C20H18N4O, 331.15533; found, 331.15497. HPLC Rt = 1.35.

N-[(1R)-1-[4-(methanesulfonylcarbamoyl)phenyl]ethyl]-1-methyl-3-phenyl-1H-pyrazole-5-carboxamide (39). 4-[(1R)-1-[(1-methyl-3-phenyl-1H-pyrazol-5-yl)formamido]ethyl]benzoic acid (15) (200 mg, 0.57 mmol), 1-hydroxy-7-azabenzotriazole (93 mg, 0.69 mmol), and 1-ethyl-3-(3-dimethylaminopropyl)-carbodiimide hydrochloride (132 mg, 0.69 mmol)were stirred for 10 min at room temperature. Methane sulfonamide (71 mg, 0.74 mmol) and N,N-diisopropylethylamine (250 µL, 1.43 mmol) were added and stirred for 16 h at room temperature. The reaction was quenched with 1 N HCl, and the mixture was concentrated in vacuo. The crude product was purified by prep. HPLC (MeCN/water) to give 39 in 50 mg (20%) yield. 1H NMR (500 MHz, DMSO-d6) δ 11.86-12.31 (m, 1H), 8.97 (d, J=7.88 Hz, 1H), 7.93 (d, J=8.20 Hz, 2H), 7.79 (dd, J=1.10, 8.04 Hz, 2H), 7.54 (d, J=8.51 Hz, 2H), 7.39-7.48 (m, 3H), 7.30-7.37 (m, 1H), 5.19 (quin, J=7.17 Hz, 1H), 4.06 (s, 3H), 1.50 (d, J=7.25 Hz, 3H), 3Hs under DMSO signal. 13C NMR (125 MHz, DMSO-d6) δ 166.7, 159.1, 150.5,

148.6, 137.1, 133.0, 130.7, 129.3, 129.1, 128.3, 126.6, 125.4, 104.9, 48.6, 43.6, 41.8, 22.4. HRMS (m/z): [M+H]+ calcd. for C21H22N4O4S , 427.14345; found, 427.14377. HPLC Rt = 0.87.

2-Methyl-5-phenyl-2H-pyrazole-3-carboxylic acid [1-(4-acetylsulfamoyl-phenyl)-ethyl]-amide (40). To 2-methyl-5-phenyl-2H-pyrazole-3-carboxylic acid [1-(4-sulfamoyl-phenyl)-ethyl]-amide (18) (50 mg, 0.13 mmol) and Et3N (75 µL, 0.52 mmol) in dry CH2Cl2 (1 mL) acetyl chloride (19 µL, 0.26 mmol) was added at 0 °C and stirred for 33 h at room temperature. The mixture was concentrated in vacuo, and the crude product was purified by prep. HPLC (MeCN/water) to give 40 in 15 mg (27%) yield. 1H NMR (400 MHz, DMSO-d6) δ 12.07 (br s, 1H), 9.00 (d, J=7.86 Hz, 1H), 7.88 (d, J=8.50 Hz, 2H), 7.78 (d, J=8.00 Hz, 2H), 7.62 (d, J=8.50 Hz, 2H), 7.40-7.43 (m, 1H), 7.39-7.48 (m, 2H), 7.33 (t, J=7.60 Hz, 1H), 5.19 (quin, J=7.16 Hz, 1H), 4.06 (s, 3H), 1.90 (s, 3H), 1.50 (d, J=7.10 Hz, 3H). 13C NMR (100 MHz, DMSO-d6) δ 169.1, 158.6, 150.2, 148.1, 138.1, 136.5, 132.5, 128.8, 127.8, 127.7, 126.6, 124.9, 104.5, 48.1, 38.9, 23.4, 21.8.

HRMS (m/z): [M+H]+ calcd. for C21H22N4O4S , 427.14345; found, 427.14360. HPLC Rt = 0.86.

[Methanesulfonyl-(4-{(R)-1-[(2-methyl-5-phenyl-2H-pyrazole-3-carbonyl)-amino]-ethyl}-phenyl)-amino]-acetic acid (41). 2-Methyl-5-phenyl-2H-pyrazole-3-carboxylic acid [(R)-1-(4-methanesulfonylamino-phenyl)-ethyl]-amide (32) (240 mg, 0.60 mmol), methyl bromo acetate (63 µL, 0.66 mmol), and K2CO3 (101 mg, 0.72 mmol) in dry MeCN (10 mL) were stirred at room temperature overnight. The mixture was partitioned between water and CH2Cl2, and the organic layer was washed with water and 1 N aqueous HCl. The organic layer was dried (Na2SO4) and concentrated in vacuo. The crude intermediate (250 mg, 0.53 mmol) and 1 N aqueous LiOH solution (2.13 mL) in THF (10 mL) were stirred at room temperature overnight. The reaction mixture was treated with water, and the pH was adjusted to 4 using 1 N aqueous HCl. The aqueous layer was extracted with EtOAc, and the combined organic layer was dried (Na2SO4) and concentrated in vacuo to give 41 in 220 mg (80%) overall yield. 1H NMR (500 MHz, DMSO-d6) δ 8.90 (d, J=8.20 Hz, 1H), 7.74-7.81 (m, 2H), 7.37-7.48 (m, 7H), 7.29-7.35

(m, 1H), 5.15 (quin, J=7.25 Hz, 1H), 4.33 (s, 2H), 4.07 (s, 3H), 3.09 (s, 3H), 1.48 (d, J=6.94 Hz, 3H), COOH not visible. 13C NMR (126 MHz, DMSO-d6) δ 170.6, 158.5, 148.1, 143.4, 139.0, 136.7, 132.6, 128.8, 127.8, 127.4, 126.8, 124.9, 104.3, 52.6, 47.7, 22.0, 2 Cs under DMSO signal. HRMS (m/z): [M+H]+ calcd. for C22H24N4O5S, 457.15402, found, 457.15314. HPLC Rt = 1.01.

(4-{1-[(2-Methyl-5-phenyl-2H-pyrazole-3-carbonyl)-amino]-ethyl}-phenyl)-acetic acid (42). The title compound was prepared according to General Method A and General Method B from 2-methyl-5-phenyl-2H-pyrazole-3-carboxylic acid (20 mg) .1H NMR (500 MHz, DMSO-d6) δ 8.85 (d, J=7.88 Hz, 1H), 7.78 (d, J=7.25 Hz, 2H), 7.37-7.46 (m, 2H), 7.37-7.40 (m, 1H), 7.29-7.34 (m, 1H), 7.28-7.36 (m, 2H), 7.21 (d, J=7.88 Hz, 2H), 5.11 (quin, J=7.17 Hz, 1H), 4.06 (s, 3H), 3.50 (s, 2H), 1.47 (q, J=6.94 Hz, 3H), COOH not visible. 13C NMR (125 MHz, DMSO-d6) δ 172.8, 158.4, 149.7, 148.1, 142.5, 136.8, 132.6, 129.3, 128.8, 127.7, 125.9, 124.9, 104.3, 77.9, 47.9, 39.0, 22.1. HRMS (m/z): [M+H]+ calcd. for C21H21N3O3 , 364.16557; found, 364.16557. HPLC Rt = 0.86.

4-{(R)-1-[(2-Methyl-5-phenyl-2H-pyrazole-3-carbonyl)-amino]-ethyl}-benzenesulfonyl)-acetic acid methyl ester (Int-10).N-[(1R)-1-(4-iodophenyl)ethyl]-1-methyl-3-phenyl-1H-pyrazole-5-carboxamide (Int-02) (420 mg, 0.97 mmol), 1,4-diazabicylco[2.2.2]octane bis(sulfur dioxide) adduct (DABSO, 271 mg, 1.07 mmol), Pd(OAc)2 (22 mg, 0.10 mmol), butyldi-1-adamantylphosphine (70 mg, 0.20 mmol), Et3N (331 µL, 2.92 mmol), and isopropanol (4 mL) were stirred for 1 h at 75 °C. Methyl bromoacetate (248 µL, 2.92 mmol) in DMF (1 mL) was added and stirred for 2 h at room temperature. The mixture was partitioned between water and EtOAc, and the organic layer was washed with water and saturated aqueous NH4Cl solution. The organic layer was dried (Na2SO4) and concentrated in vacuo. The crude product was purified by MPLC (cyclohexane/EtOAc) to give Int-10 in 330 mg (79%) yield. 1H NMR (500 MHz, DMSO-d6) δ 9.02 (d, J=7.57 Hz, 1H), 7.89 (d, J=8.51 Hz, 2H), 7.79 (d, J=7.25 Hz, 2H), 7.68 (d, J=8.51 Hz, 2H), 7.41-7.47 (m, 3H), 7.34 (t, J=7.60 Hz, 1H), 5.22 (quin, J=7.25 Hz, 1H), 4.64 (s, 2H), 4.06 (s, 3H), 3.59 (s, 3H), 1.51 (d, J=7.25 Hz, 3H). 13C NMR (126 MHz, DMSO-d6) δ 163.2, 158.7, 151.1, 148.1, 137.4, 136.5, 132.5, 128.8, 128.4, 127.8,

126.8, 124.9, 104.5, 59.5, 52.5, 48.2, 21.9, 1 C under DMSO signal. HRMS (m/z): [M+H]+ calcd. for C22H23N3O5S, 442.14312, found, 442.14279. HPLC Rt = 1.30.

(4-{(R)-1-[(2-Methyl-5-phenyl-2H-pyrazole-3-carbonyl)-amino]-ethyl}-benzenesulfonyl)-acetic acid (43). The title compound was prepared from Int-10 (98 mg, 0.22 mmol) according to General Method B in 89 mg (93%) yield.

4-{(R)-1-[(1-Methyl-1H-indole-2-carbonyl)-amino]-ethyl}-benzoic acid (44). The title compound was prepared according to General Method A and General Method B from 1-methylindole-2-carboxylic acid (50 mg, 0.29 mmol) in 55 mg (61%) yield. 1H NMR (500 MHz, DMSO-d6) δ 12.27-13.33 (m, 1H), 8.94 (d, J=7.88 Hz, 1H), 7.91 (d, J=8.51 Hz, 2H), 7.65 (d, J=7.88 Hz, 1H), 7.45-7.56 (m, 3H), 7.22-7.30 (m, 2H), 7.10 (t, J=7.30 Hz, 1H), 5.21 (quin, J=7.25 Hz, 1H), 3.94 (s, 3H), 1.50 (d, J=7.25 Hz, 3H). 13C NMR (125 MHz, DMSO-d6) δ 167.2, 161.2, 150.0, 138.4, 131.9, 129.4, 129.2, 126.2, 125.5, 123.6, 121.5, 120.1, 110.5, 104.7, 48.1, 31.3, 22.0. HRMS (m/z): [M+H]+ calcd. for C19H18N2O3, 323.13902; found, 323.13939. HPLC Rt = 0.85.

4-{(R)-1-[(5-Chloro-1-methyl-1H-indole-2-carbonyl)-amino]-ethyl}-benzoic acid (45).

The title compound was prepared according to General Method A and General Method B from 5-chloro-1-methyl-1H-indole-2-carboxylic acid (60 mg, 0.29 mmol) in 93 mg (91%) yield. 1H NMR (500 MHz, DMSO-d6) δ 12.86 (br s, 1H), 9.03 (br d, J=7.88 Hz, 1H), 7.92 (br d, J=8.20 Hz, 2H), 7.74 (s, 1H), 7.57 (br d, J=8.83 Hz, 1H), 7.52 (br d, J=7.88 Hz, 2H), 7.27 (dd, J=1.42, 8.67 Hz, 1H), 7.22 (s, 1H), 5.20 (quin, J=7.09 Hz, 1H), 3.93 (s, 3H), 1.50 (br d, J=7.25 Hz, 3H). 13C NMR (125 MHz, DMSO-d6) δ 167.2, 160.8, 149.9, 136.9, 133.3, 129.5, 129.2, 126.5, 126.2, 124.6, 123.6, 120.6, 112.3, 104.2, 48.2, 31.6, 22.0. HRMS (m/z): [M+H]+ calcd. for C19H17ClN2O3 , 357.10005; found, 357.10038. HPLC Rt = 0.90.

4-{(R)-1-[(5-Chloro-7-methoxy-1-methyl-1H-indole-2-carbonyl)-amino]-ethyl}-benzoic acid (46). The title compound was prepared according to General Method A and General Method B from 5-chloro-7-methoxy-1-methylindole-2-carboxylic acid (70 mg, 28 mmol) in 96 mg (88%) yield. 1H NMR (500 MHz, DMSO-d6) δ 9.01 (d, J=7.88 Hz, 1H), 7.91 (d, J=8.20 Hz, 2H), 7.51 (d, J=8.20 Hz, 2H), 7.27 (d, J=1.89 Hz, 1H), 7.07 (s, 1H),

6.76 (d, J=1.58 Hz, 1H), 5.17 (quin, J=7.17 Hz, 1H), 4.12 (s, 3H), 3.90 (s, 3H), 1.48 (d, J=6.94 Hz, 3H), COOH not visible. 13C NMR (125 MHz, DMSO-d6) δ 167.3, 160.8, 149.9, 148.3, 134.0, 129.5, 129.3, 128.0, 126.6, 126.2, 124.7, 113.2, 105.3, 105.0, 56.2, 48.3, 34.4, 22.0. HRMS (m/z): [M+H]+ calcd. for C20H19ClN2O4 , 387.11061; found, 387.11098. HPLC Rt = 0.98.

4-{(R)-1-[(5-Chloro-1-methyl-7-trifluoromethoxy-1H-indole-2-carbonyl)-amino]-ethyl}-benzoic acid (47). The title compound was prepared according to General Method A and General Method B from 5-chloro-1-methyl-7-trifluoromethoxy-1H-indole-2-carboxylic acid (40 mg, 0.13 mmol) in 56 mg yield. 1H NMR (400 MHz, DMSO-d6) δ 9.19 (d, J=7.86 Hz, 1H), 7.92 (d, J=8.36 Hz, 2H), 7.85 (d, J=1.77 Hz, 1H), 7.52 (d, J=8.36 Hz, 2H), 7.29-7.35 (m, 1H), 7.24 (s, 1H), 5.19 (quin, J=7.16 Hz, 1H), 4.05 (s, 3H), 1.49 (d, J=7.10 Hz, 3H), COOH not visible. 13C NMR (100 MHz, DMSO-d6) δ 167.2, 160.2, 149.6, 135.9, 134.5, 130.0, 129.5, 129.3, 128.1, 126.2, 123.6, 120.6, 120.2 (q, J(CF)=257.5 Hz,), 116.4, 105.3, 48.3, 33.6, 21.9. HRMS (m/z): [M+H]+ calcd. for C20H16ClF3N2O4, 441.08235; found, 441.08145. HPLC Rt = 1.09.

4-{(R)-1-[(6-Bromo-5-chloro-1-methyl-1H-indole-2-carbonyl)-amino]-ethyl}-benzoic acid (48). The title compound was prepared according to General Method A and General Method B from 6-bromo-5-chloro-1-methylindole-2-carboxylic acid in 20 mg yield. 1H NMR (400 MHz, DMSO-d6) δ 9.09 (d, J=7.86 Hz, 1H), 8.03 (s, 1H), 7.96 (s, 1H), 7.91 (d, J=8.36 Hz, 2H), 7.51 (d, J=8.36 Hz, 2H), 7.21 (s, 1H), 5.19 (quin, J=7.22 Hz, 1H), 3.91 (s, 3H), 1.49 (d, J=7.10 Hz, 3H) acid OH not visible. 13C NMR (100 MHz, DMSO-d6) δ 167.3, 160.6, 149.7, 137.6, 134.1, 129.5, 129.5, 126.2, 125.9, 124.4, 122.4, 116.0, 115.8, 104.4, 48.3, 31.9, 22.0. HRMS (m/z): [M+H]+ calcd. for C19H16BrClN2O3, 435.01056; found, 435.01065. HPLC Rt = 1.11.

4-{(R)-1-[(3-Methyl-3H-benzo[e]indole-2-carbonyl)-amino]-ethyl}-benzoic acid (49). The title compound was prepared according to General Method A and General Method B from 3-methyl-3H-benzo[e]indole-2-carboxylic acid (90 mg, 0.28 mmol) in 90 mg (86%) yield. 1H NMR (500 MHz, DMSO-d6) δ 8.96 (d, J=7.88 Hz, 1H), 8.24 (d, J=8.20 Hz, 1H), 7.90-8.00 (m, 3H), 7.88 (s, 1H), 7.74 (s, 2H), 7.51-7.64 (m, 3H), 7.45 (t, J=7.25 Hz, 1H), 5.24 (quin, J=7.17 Hz, 1H), 4.07 (s, 3H), 1.54 (d, J=6.94 Hz, 3H), COOH not

visible. 13C NMR (125 MHz, DMSO-d6) δ 167.2, 161.1, 150.0, 135.4, 130.0, 129.4, 129.3, 128.9, 128.7, 128.0, 126.4, 126.2, 124.7, 123.8, 122.4, 120.5, 112.1, 104.3, 48.1, 31.8, 22.1. HRMS (m/z): [M+H]+ calcd. for C23H20N2O3, 373.15467; found, 373.15503. HPLC Rt = 0.96.

4-{(R)-1-[(5-Chloro-1,6-dimethyl-1H-indole-2-carbonyl)-amino]-ethyl}-benzoic acid (50). The title compound was prepared according to General Method A and General Method B from 5-chloro-1,6-dimethyl-1H-indole-2-carboxylic acid (218 mg, 0.57 mmol) in 193 mg (92%) yield. 1H NMR (500 MHz, DMSO-d6) δ 12.21-13.49 (m, 1H), 8.98 (d, J=8.20 Hz, 1H), 7.91 (d, J=8.20 Hz, 2H), 7.73 (s, 1H), 7.47-7.58 (m, 3H), 7.18 (s, 1H), 5.19 (quin, J=7.25 Hz, 1H), 3.90 (s, 3H), 2.44 (s, 3H), 1.49 (d, J=7.25 Hz, 3H). 13C NMR (125 MHz, DMSO-d6) δ 167.2, 160.9, 149.9, 137.4, 132.6, 130.5, 129.4, 129.2, 126.2, 125.9, 124.8, 120.9, 112.3, 104.1, 48.1, 31.5, 22.0, 20.7. HRMS (m/z): [M+H]+ calcd. for C20H19ClN2O3, 371.11570; found, 371.11551. HPLC Rt = 1.00.

4-{(R)-1-[(4,5-Dichloro-1-methyl-1H-indole-2-carbonyl)-amino]-ethyl}-benzoic acid (51). The title compound was prepared according to General Method A and General

Method B from 4,5-dichloro-1-methyl-1H-indole-2-carboxylic acid (50 mg, 0.21 mmol) in 35 mg (44%) yield. 1H NMR (400 MHz, DMSO-d6) δ 9.15 (d, J=7.86 Hz, 1H), 7.92 (d, J=8.36 Hz, 2H), 7.60 (d, J=8.87 Hz, 1H), 7.53 (d, J=8.36 Hz, 2H), 7.44 (d, J=8.87 Hz, 1H), 7.36 (s, 1H), 5.20 (quin, J=7.16 Hz, 1H), 3.96 (s, 3H), 1.51 (d, J=7.10 Hz, 3H), COOH not visible. 13C NMR (100 MHz, DMSO-d6) δ 167.2, 160.3, 149.8, 137.3, 133.7, 129.5, 129.3, 126.2, 125.4, 124.8, 123.0, 122.6, 111.4, 103.1, 48.3, 32.1, 22.0. HRMS (m/z): [M+H]+ calcd. for C19H16Cl2N2O3, 391.06107; found, 391.06168. HPLC Rt = 1.01.

4-{(R)-1-[(4-Chloro-1,6-dimethyl-1H-indole-2-carbonyl)-amino]-ethyl}-benzoic acid (52). The title compound was prepared according to General Method A and General Method B from 4-chloro-1,6-dimethyl-1H-indole-2-carboxylic acid (229 mg, 1.02 mmol) in 287 mg (76%) yield. 1H NMR (400 MHz, DMSO-d6) δ 11.97-13.66 (m, 1H), 9.03 (br d, J=7.60 Hz, 1H), 7.92 (br d, J=7.60 Hz, 2H), 7.52 (br d, J=7.60 Hz, 2H), 7.31 (br d, J=13.69 Hz, 2H), 7.05 (br s, 1H), 5.19 (br t, J=6.72 Hz, 1H), 3.92 (br s, 3H), 2.43 (br s, 3H), 1.50 (br d, J=6.34 Hz, 3H). 13C NMR (100 MHz, DMSO-d6) δ 167.2, 160.7, 150.0,

139.5, 134.4, 132.0, 129.5, 129.2, 126.2, 125.2, 122.1, 121.4, 109.6, 102.8, 48.2, 31.8, 22.0, 21.4. HRMS (m/z): [M+H]+ calcd. for C20H19ClN2O3 , 371.11570; found, 371.11584. HPLC Rt = 1.04.

4-{(R)-1-[(4-Chloro-5-fluoro-7-methoxy-1-methyl-1H-indole-2-carbonyl)-amino]-ethyl}-benzoic acid (55). The title compound was prepared according to General Method A and General Method B from 4-chloro-5-fluoro-7-methoxy-1-methylindole-2-carboxylic acid (50 mg, 19 mmol) in 40 mg (53%) yield. 1H NMR (500 MHz, DMSO-d6) δ 12.50-13.30 (m, 1H), 9.09 (br d, J=7.88 Hz, 1H), 7.92 (d, J=8.51 Hz, 2H), 7.52 (d, J=8.51 Hz, 2H), 7.23 (s, 1H), 6.90 (d, J=11.98 Hz, 1H), 5.18 (quin, J=7.17 Hz, 1H), 4.09-4.20 (m, 3H), 3.92 (s, 3H), 1.49 (d, J=6.94 Hz, 3H). 13C NMR (125 MHz, DMSO-d6) δ ppm 167.2 160.3, 152.2 (d, J(CF)=237.1 Hz) 150.3, 149.7, 147.3 (d, J(CF)=10.9 Hz) 134.4 (d, J(CF)=4.7 Hz) 129.5, 129.4, 129.3, 126.4, 126.2, 125.3 (d, J(CF)=3.6 Hz) 124.8, 103.5 (br d, J(CF)=5.5 Hz) 101.0 (d, J(CF)=20.0 Hz) 95.7 (br d, J(CF)=30.0 Hz) 56.6, 48.3, 34.5, 21.9 . HRMS (m/z): [M+H]+ calcd. for C20H18ClFN2O4, 405.10119; found, 405.10132. HPLC Rt = 1.00.

Methyl (2Z)-2-azido-3-(2,3-dichloro-4-methylphenyl)prop-2-enoate (Int-05). Sodium (134 mg, 5.82 mmol) was slowly added to dry MeOH (10 mL). A mixture of 2,3-Dichloro-4-methylbenzaldehyde (500 mg, 2.65 mmol) and ethyl -2-azido acetate (30% in CH_2Cl_2, 5.69 g, 13.23 mmol) are added at – 78 °C and stirred for 1 h. The mixture is brought to room temperature and stirred overnight. The mixture was partitioned between water and EtOAc, and the organic layer was washed with water and saturated aqueous NaCl solution. The organic layer was dried (Na2SO4) and concentrated in vacuo to give Int-05 as a yellow solid in 618 mg (82%) yield.

Methyl 4,5-dichloro-6-methyl-1H-indole-2-carboxylate (Int-06). Methyl (2Z)-2-azido-3-(2,3-dichloro-4-methylphenyl)prop-2-enoate (Int-05) (618 mg, 2.16 mmol) in o-xylene (10 mL) was stirred for 50 min at 130 °C. The reaction solution was concentrated in vacuo to provide the product Int-06 in 595 mg (96%) yield.

Methyl 4,5-dichloro-1,6-dimethyl-1H-indole-2-carboxylate (Int-07). Methyl 4,5-dichloro-6-methyl-1H-indole-2-carboxylate (Int-06) (1.97 g, 7.62 mmol), K2CO3 (2.21 g, 16.00 mmol), and iodomethane (1.64 g, 11.43 mmol) in dry DMF (20 mL) were stirred for 1 h

at 60 °C. The solid was filtered off, and the filtrate was treated with water. The precipitate was filtered off, washed with water and dried to provide the product Int-07 as white solid in 2.03 g (98%) yield.

4,5-dichloro-1,6-dimethyl-1H-indole-2-carboxylic acid (Int-08). To methyl 4,5-dichloro-1,6-dimethyl-1H-indole-2-carboxylate (Int-07) (2.03 g, 7.46 mmol) in MeOH (50 mL) 8 M aqueous NaOH (2.0 mL, 16.0 mmol) was added and stirred for 1 h at 65°C. The solvent was removed in vacuo, and the residue was treated with with 2 N HCl. The precipitate was filtered off, washed with water and dried to provide the product Int-08 as white solid in 1.91 g (99%) yield.

All other 1-methyl-1H-indole-2-carboxylic acids were prepared in an analogous way from commercially available starting materials.

4-[(1R)-1-[(4,5-dichloro-1,6-dimethyl-1H-indol-2-yl)formamido]ethyl]benzoic acid (57). The title compound was prepared according to General Method A and General Method B from 4,5-dichloro-1,6-dimethyl-1H-indole-2-carboxylic acid (2 mg, 0.19 mmol) in 79 mg (quant.) yield. 1H NMR (500 MHz, DMSO-d6) δ 9.10 (d, J=7.57 Hz, 1H), 7.92 (d,

J=8.20 Hz, 2H), 7.59 (s, 1H), 7.52 (d, J=8.20 Hz, 2H), 7.31 (s, 1H), 5.20 (quin, J=7.17 Hz, 1H), 3.94 (s, 3H), 1.50 (d, J=7.25 Hz, 3H), 3H under DMSO, acid OH not visible. 13C NMR (125 MHz, DMSO-d6) δ 167.2, 160.4, 149.8, 136.9, 132.9, 132.2, 129.5, 129.3, 126.2, 123.7, 123.6, 123.3, 111.4, 103.1, 48.3, 31.9, 21.9, 21.6. HRMS (m/z): [M+H]+ calcd. for C20H18Cl2N2O3, 405.07672; found, 405.07687. HPLC Rt = 1.07.

2-{4-[(1R)-1-[(4,5-dichloro-1,6-dimethyl-1H-indol-2-yl)formamido]ethyl]benzenesulfonyl}acetic acid (58). The title compound was prepared as described for the synthesis of 2-{4-[(1S)-1-[(4,5-dichloro-1,6-dimethyl-1H-indol-2-yl)formamido]-2-hydroxyethyl]benzenesulfonyl}acetic acid (BI-4924). 1H NMR (400 MHz, DMSO-d6) δ 13.04-13.52 (m, 1H), 9.14 (d, J=7.60 Hz, 1H), 7.89 (d, J=8.36 Hz, 2H), 7.67 (d, J=8.36 Hz, 2H), 7.60 (s, 1H), 7.34 (s, 1H), 5.23 (quin, J=7.16 Hz, 1H), 4.43 (s, 2H), 3.94 (s, 3H), 1.51 (d, J=7.10 Hz, 3H), 3 Hs under DMSO signal. 13C NMR (100 MHz, DMSO-d6) δ 163.9, 160.4, 151.0, 137.8, 136.9, 132.8, 132.2, 128.3, 126.7, 123.7, 123.6, 123.3, 111.4, 103.2, 60.2, 48.2, 31.9, 21.9, 21.6. HRMS (m/z): [M+H]+ calcd. for

C21H20Cl2N2O5S , 439.06444; found, 439.06381 (in source fragmentation –CO2). HPLC Rt = 1.10.

2-{4-[(1R)-1-[(4-chloro-1,6-dimethyl-1H-indol-2-yl)formamido]ethyl]benzenesulfonyl}acetic acid (59). The title compound was prepared as described for the synthesis of 2-{4-[(1S)-1-[(4,5-dichloro-1,6-dimethyl-1H-indol-2-yl)formamido]-2-hydroxyethyl]benzenesulfonyl}acetic acid (BI-4924). 1H NMR (400 MHz, DMSO-d6) δ 12.91-13.62 (m, 1H), 9.07 (d, J=7.60 Hz, 1H), 7.89 (d, J=8.11 Hz, 2H), 7.67 (d, J=8.36 Hz, 2H), 7.32 (d, J=7.86 Hz, 2H), 7.05 (s, 1H), 5.23 (quin, J=7.16 Hz, 1H), 4.46 (s, 2H), 3.93 (s, 3H), 2.43 (s, 3H), 1.51 (d, J=6.84 Hz, 3H). 13C NMR (100 MHz, DMSO-d6) δ 164.0, 160.7, 151.2, 139.5, 137.7, 134.4, 131.8, 128.3, 126.7, 125.1, 122.1, 121.4, 109.5, 102.9, 60.0, 48.2, 31.8, 22.0, 21.3. HRMS (m/z): [M+H]+ calcd. for C21H21ClN2O5S, 449.09325, found, 449.09274. HPLC Rt = 1.13.

5-Chloro-1-methyl-1H-indole-2-carboxylic acid (2-hydroxy-1-phenyl-ethyl)-amide (60). The title compound was prepared according to General Method A from 5-chloro-1-methyl-1H-indole-2-carboxylic acid (70 mg, 0.32 mmol) in 80 mg (76%) yield. 1H NMR

(500 MHz, DMSO-d6) δ 8.84 (d, J=8.20 Hz, 1H), 7.74 (d, J=1.89 Hz, 1H), 7.56 (d, J=8.83 Hz, 1H), 7.40 (d, J=7.57 Hz, 2H), 7.33 (t, J=7.57 Hz, 2H), 7.20-7.29 (m, 3H), 5.06 (dt, J=5.83, 7.96 Hz, 1H), 4.97 (t, J=5.83 Hz, 1H), 3.93 (s, 3H), 3.60-3.76 (m, 2H). 13C NMR (125 MHz, DMSO-d6) δ 161.3, 141.2, 136.8, 133.6, 128.2, 127.0, 126.9, 126.6, 124.6, 123.5, 120.5, 112.3, 104.2, 64.5, 55.7, 31.6. HRMS (m/z): [M+H]+ calcd. for C18H17ClN2O2, 329.10513; found, 329.10558. HPLC Rt = 1.28.

[(5-Chloro-1-methyl-1H-indole-2-carbonyl)-amino]-phenyl-acetic acid (61). The title compound was prepared according to General Method A and General Method B from 5-chloro-1-methyl-1H-indole-2-carboxylic acid (70 mg, 0.32 mmol) in 59 mg (63%) yield. 1H NMR (500 MHz, DMSO-d6) δ 12.96 (br s, 1H), 9.16 (d, J=7.57 Hz, 1H), 7.72 (d, J=1.89 Hz, 1H), 7.58 (d, J=9.14 Hz, 1H), 7.51 (d, J=7.20 Hz, 2H), 7.39 (t, J=7.20 Hz, 2H), 7.34 (t, J=7.20 Hz, 1H), 7.23-7.30 (m, 2H), 5.60 (d, J=7.57 Hz, 1H), 3.96 (s, 3H). 13C NMR (125 MHz, DMSO-d6) δ 171.8, 161.3, 136.9, 136.9, 132.7, 128.4, 128.2, 128.0, 126.5, 124.6, 123.7, 120.7, 112.3, 105.0, 56.4, 31.7. HRMS (m/z): [M+H]+ calcd. for C18H15ClN2O3, 343.08440; found, 343.08392. HPLC Rt = 0.93.

5-Chloro-N-(3-hydroxy-1-phenylpropyl)-1-methyl-1H-indole-2-carboxamide (62). The title compound was prepared according to General Method A from 5-chloro-1-methyl-1H-indole-2-carboxylic acid (70 mg, 0.32 mmol) in 60 mg (55%) yield. 1H NMR (500 MHz, DMSO-d6) δ 8.92 (d, J=8.20 Hz, 1H), 7.74 (d, J=1.89 Hz, 1H), 7.56 (d, J=8.83 Hz, 1H), 7.40 (d, J=7.70 Hz, 2H), 7.33 (t, J=7.72 Hz, 2H), 7.26 (dd, J=2.21, 8.83 Hz, 1H), 7.23 (t, J=7.30 Hz, 1H), 7.17 (s, 1H), 5.15 (dt, J=6.15, 8.43 Hz, 1H), 4.60 (t, J=4.89 Hz, 1H), 3.92 (s, 3H), 3.38-3.54 (m, 2H), 2.03 (br dd, J=5.52, 8.35 Hz, 1H), 1.76-1.95 (m, 1H). 13C NMR (125 MHz, DMSO-d6) δ 160.9, 143.9, 136.8, 133.6, 128.3, 126.7, 126.6, 126.5, 124.6, 123.5, 120.5, 112.3, 104.0, 57.8, 50.0, 38.9, 31.5. HRMS (m/z): [M+H]+ calcd. for C19H19ClN2O2, 343.12078; found, 343.12134. HPLC Rt = 1.28.

5-Chloro-1-methyl-1H-indole-2-carboxylic acid (2-methoxy-1-phenyl-ethyl)-amide (63). The title compound was prepared according to General Method A from 5-chloro-1-methyl-1H-indole-2-carboxylic acid (70 mg, 0.32 mmol) in 80 mg (73%) yield. 1H NMR (500 MHz, DMSO-d6) δ 8.98 (d, J=8.20 Hz, 1H), 7.75 (d, J=1.89 Hz, 1H), 7.57 (d, J=8.83 Hz, 1H), 7.43 (d, J=7.57 Hz, 2H), 7.35 (t, J=7.57 Hz, 2H), 7.23-7.29 (m, 2H),

7.21 (s, 1H), 5.26 (dt, J=5.36, 8.51 Hz, 1H), 3.94 (s, 3H), 3.69 (t, J=1.00 Hz, 1H), 3.55 (dd, J=5.36, 10.09 Hz, 1H), 3.31 (s, 3H). 13C NMR (125 MHz, DMSO-d6) δ 161.1, 140.5, 136.8, 133.4, 128.3, 127.2, 127.0, 126.5, 124.6, 123.5, 120.6, 112.3, 104.2, 74.5, 58.0, 52.3, 31.6. HRMS (m/z): [M+H]+ calcd. for C19H19ClN2O2, 343.12078; found, 343.11996. HPLC Rt = 1.41.

5-Chloro-1-methyl-1H-indole-2-carboxylic acid (2-amino-1-phenyl-ethyl)-amide (64).

The title compound was prepared according to General Method A from 5-chloro-1-methyl-1H-indole-2-carboxylic acid (70 mg, 0.32 mmol) and (2-amino-2-phenyl-ethyl)-carbamic acid tert-butyl ester (124 mg, 0.50 mmol) with subsequent boc deprotection in 24 mg (23%) yield. 1H NMR (500 MHz, DMSO-d6) δ 9.06 (br d, J=8.51 Hz, 1H), 7.82-8.16 (m, 2H), 7.77 (d, J=1.89 Hz, 1H), 7.59 (d, J=8.83 Hz, 1H), 7.45 (d, J=7.30 Hz, 2H), 7.40 (t, J=7.57 Hz, 2H), 7.24-7.35 (m, 3H), 5.26-5.37 (m, 1H), 3.95 (s, 3H), 3.17-3.30 (m, 2H). 13C NMR (125 MHz, DMSO-d6) δ 161.6, 139.7, 136.9, 133.1, 128.7, 127.8, 126.7, 126.4, 124.8, 123.8, 120.6, 112.4, 104.7, 51.1, 43.1, 31.6. HRMS (m/z): [M+H]+ calcd. for C18H18ClN3O, 328.12112; found, 328.12151. HPLC Rt = 1.22.

5-Chloro-1-methyl-1H-indole-2-carboxylic acid (carbamoyl-phenyl-methyl)-amide (65).

The title compound was prepared according to General Method A from 5-chloro-1-methyl-1H-indole-2-carboxylic acid (70 mg, 0.32 mmol) in 91 mg (83%) yield. 1H NMR (500 MHz, DMSO-d6) δ 8.80 (d, J=7.88 Hz, 1H), 7.66-7.74 (m, 2H), 7.57 (d, J=9.14 Hz, 1H), 7.53 (d, J=7.57 Hz, 2H), 7.37 (t, J=7.60 Hz, 2H), 7.29-7.33 (m, 1H), 7.26 (s, 3H), 5.61 (d, J=7.88 Hz, 1H), 3.94 (s, 3H). 13C NMR (125 MHz, DMSO-d6) δ 171.5, 161.0, 138.6, 136.9, 133.0, 128.3, 127.6, 127.5, 126.6, 124.6, 123.6, 120.7, 112.3, 104.8, 56.5, 31.6. HRMS (m/z): [M+H]+ calcd. for C18H16ClN3O2, 342.10038; found, 342.10095. HPLC Rt = 1.21.

5-Chloro-1-methyl-1H-indole-2-carboxylic acid ((1S,2R)-2-hydroxy-1-phenyl-propyl)-amide (66) and **5-chloro-1-methyl-1H-indole-2-carboxylic acid ((1S,2S)-2-hydroxy-1-phenyl-propyl)-amide (67)**. The title compounds were prepared according to General Method A from 5-chloro-1-methyl-1H-indole-2-carboxylic acid (65 mg, 0.31 mmol) with subsequent SFC separation of the diastereomeric product mixture.

66: ^{1}H NMR (400 MHz, DMSO-d_6) δ 8.69 (br d, *J*=8.11 Hz, 1H), 7.74 (br s, 1H), 7.56 (br d, *J*=8.62 Hz, 1H), 7.42 (br d, *J*=7.10 Hz, 2H), 7.17-7.36 (m, 5H), 4.84 (br d, *J*=4.31 Hz, 2H), 3.94-4.05 (m, 1H), 3.91 (br s, 3H), 0.93-1.06 (m, 3H). ^{13}C NMR (100 MHz, DMSO-d_6) δ 161.2, 141.8, 136.8, 133.8, 128.1, 127.5, 126.8, 126.6, 124.6, 123.4, 120.5, 112.3, 104.1, 68.7, 59.9, 31.5, 20.9. HRMS (*m/z*): $[M+H]^+$ calcd. for $C_{19}H_{19}ClN_2O_2$, 343.12078; found, 343.12103. HPLC Rt = 1.31.

67: ^{1}H NMR (400 MHz, DMSO-d_6) δ 8.76 (d, *J*=8.87 Hz, 1H), 7.74 (d, *J*=2.03 Hz, 1H), 7.56 (d, *J*=8.87 Hz, 1H), 7.42 (d, *J*=7.35 Hz, 2H), 7.31 (t, *J*=7.48 Hz, 2H), 7.19-7.28 (m, 2H), 7.16 (s, 1H), 4.85 (t, *J*=7.98 Hz, 1H), 4.79 (d, *J*=5.83 Hz, 1H), 4.00 (sxt, *J*=6.24 Hz, 1H), 3.91 (s, 3H), 1.14 (d, *J*=6.34 Hz, 3H). ^{13}C NMR (100 MHz, DMSO-d_6) δ 160.9, 141.3, 136.9, 133.7, 128.1, 127.8, 126.7, 126.6, 124.7, 123.6, 120.6, 112.3, 104.1, 68.4, 59.1, 31.6, 20.8. HRMS (*m/z*): $[M+H]^+$ calcd. for $C_{19}H_{19}ClN_2O_2$, 343.12078; found, 343.12135. HPLC Rt = 1.29.

5-Chloro-1-methyl-1H-indole-2-carboxylic acid ((trans)-3,3,3-trifluoro-2-hydroxy-1-phenyl-propyl)-amide (68). The title compound was prepared according to General

Method A from 5-chloro-1-methyl-1H-indole-2-carboxylic acid (25 mg, 0.12 mmol) in 40 mg (85%) yield. ^{1}H NMR (500 MHz, DMSO-d_6) δ 9.07 (d, *J*=9.46 Hz, 1H), 7.77 (d, *J*=1.89 Hz, 1H), 7.56 (d, *J*=8.83 Hz, 1H), 7.51 (d, *J*=7.57 Hz, 2H), 7.36 (t, *J*=7.60 Hz, 2H), 7.24-7.32 (m, 2H), 7.10 (s, 1H), 6.36-6.56 (m, 1H), 5.27 (t, *J*=9.46 Hz, 1H), 4.42 (br s, 1H), 3.91 (s, 3H). ^{13}C NMR (125 MHz, DMSO-d_6) δ 160.3, 139.7, 136.8, 133.1, 128.4, 128.1, 127.4, 126.4, 124.8, 123.7, 125.6(q, *J(CF)*=284.6 Hz,), 120.6, 112.4, 104.2, 69.5 (q, *J(CF)*=27.9 Hz,), 52.4, 31.5. HRMS (*m/z*): $[M+H]^+$ calcd. for $C_{19}H_{16}ClF_3N_2O_2$, 397.09252; found, 397.09347. HPLC Rt = 1.39.

5-Chloro-1-methyl-1H-indole-2-carboxylic acid ((cis)-3,3,3-trifluoro-2-hydroxy-1-phenyl-propyl)-amide (69). The title compound was prepared according to General Method A from 5-chloro-1-methyl-1H-indole-2-carboxylic acid (25 mg, 0.12 mmol) in 39 mg (82%) yield. ^{1}H NMR (400 MHz, DMSO-d_6) δ 8.86 (d, *J*=9.38 Hz, 1H), 7.77 (d, *J*=1.77 Hz, 1H), 7.57 (d, *J*=8.87 Hz, 1H), 7.53 (d, *J*=7.60 Hz, 2H), 7.37 (t, *J*=7.60 Hz, 2H), 7.24-7.32 (m, 2H), 7.19 (s, 1H), 6.57-6.83 (m, 1H), 5.48 (dd, *J*=4.18, 9.25 Hz, 1H), 4.40-4.46 (m, 1H), 3.92 (s, 3H). ^{13}C NMR (100 MHz, DMSO-d_6) δ 160.9, 139.4, 136.9,

133.2, 128.3, 127.5, 126.5, 126.5, 124.7, 123.7, 120.7, 112.3, 104.5, 71.2(q, *J(CF)*=28.5 Hz,), 51.9, 31.5, CF_3 not visible. HRMS (*m/z*): $[M+H]^+$ calcd. for $C_{19}H_{16}ClF_3N_2O_2$, 397.09252; found, 397.08277. HPLC Rt = 1.42.

4,5-Dichloro-N-[(1S)-2-hydroxy-1-(4-iodophenyl)ethyl]-1,6-dimethyl-1H-indole-2-carboxamide (Int-09). To 4,5-dichloro-1,6-dimethyl-1H-indole-2-carboxylic acid (**Int-08**) (1.00 g, 3.87 mmol) and HATU (1.77 g, 4.65 mmol) in MeCN (15 mL) iPr2NEt (1.68 mL, 9.69 mmol) was added and stirred for 10 min at room temperature. (2S)-2-Amino-2-(4-iodophenyl)ethan-1-ol hydrochloride (1.22 g, 6.07 mmol) was added and stirred for 1 h at room temperature. Water was added to the reaction mixture, and the precipitate was filtered off, washed with water and dried to provide the product **Int-09** as white solid in 2.00 g (97%) yield.

Ethyl 2-{4-[(1S)-1-[(4,5-dichloro-1,6-dimethyl-1H-indol-2-yl)formamido]-2-hydroxyethyl]benzenesulfonyl}acetate (BI-4916). The title compound was prepared from 4,5-dichloro-N-[(1S)-2-hydroxy-1-(4-iodophenyl)ethyl]-1,6-dimethyl-1H-indole-2-carboxamide (**Int-09**) (2.00 g, 3.98 mmol) as described for **Int-10** in 1.32 g (63%) yield.

^{1}H NMR (500 MHz, DMSO-d_6) δ 9.04 (d, *J*=7.88 Hz, 1H), 7.89 (d, *J*=8.40 Hz, 2H), 7.69 (d, *J*=8.40 Hz, 2H), 7.59 (s, 1H), 7.36 (s, 1H), 5.08-5.20 (m, 2H), 4.59 (s, 2H), 4.01 (q, *J*=7.25 Hz, 2H), 3.93 (s, 3H), 3.65-3.81 (m, 2H), 1.02 (t, *J*=7.09 Hz, 3H), 3 Hs under DMSO signal. ^{13}C NMR (125 MHz, DMSO-d_6) δ 162.7, 161.0, 147.8, 137.6, 137.0, 132.9, 132.3, 128.2, 127.9, 123.8, 123.6, 123.4, 111.5, 103.3, 64.0, 61.5, 59.8, 55.6, 31.9, 21.6, 13.7. HRMS (*m/z*): $[M+H]^+$ calcd. for $C_{23}H_{24}Cl_2N_2O_6S$, 527.08049; found, 527.08060. HPLC Rt = 1.38. The purity of BI-4916 is > 95% according to HPLC analysis (for HPLC traces see Supporting Information).

2-{4-[(1S)-1-[(4,5-Dichloro-1,6-dimethyl-1H-indol-2-yl)formamido]-2-hydroxyethyl]benzenesulfonyl}acetic acid (BI-4924). 8 M aqueous NaOH (0.40 mL, 3.20 mmol) was added to **BI-4916** (267 mg, 0.52 mmol) in MeCN (1 mL) and stirred for 30 min at 70 °C. The mixture was treated with 2 N HCl, and the precipitate was filtered off, washed with water and dried to provide the product **BI-4924** as white solid in 23 mg (36%) yield. ^{1}H NMR (400 MHz, DMSO-d_6) δ 9.06 (d, *J*=7.86 Hz, 1H), 7.89 (d, *J*=8.36 Hz, 2H), 7.68 (d, *J*=8.36 Hz, 2H), 7.61 (s, 1H), 7.37 (s, 1H), 5.06-5.21 (m, 2H), 4.46 (s,

2H), 3.94 (s, 3H), 3.66-3.76 (m, 2H), acid OH not visible, 3 Hs under DMSO signal. ^{13}C NMR (125 MHz, DMSO-d_6) δ 164.0, 161.0, 147.5, 138.1, 137.0, 132.8, 132.3, 128.1, 127.8, 123.7, 123.6, 123.4, 111.5, 103.3, 64.0, 60.1, 55.5, 31.9, 21.6. HRMS (*m/z*): $[M+H]^+$ calcd. for $C_{21}H_{20}Cl_2N_2O_6S$, 455.05936; found, 455.05991 (in source fragmentation $–CO_2$). HPLC Rt = 1.01. The purity of BI-4924 is > 95% according to HPLC analysis (for HPLC traces see Supporting Information).

AUTHOR INFORMATION

Corresponding Author

*H.W.: e-mail, harald.weinstabl@boehringer-ingelheim.com; phone, +43-1-80105-2803

Author Contributions

The manuscript was written through contributions of all authors. All authors have given approval to the final version of the manuscript. ‡These authors contributed equally.

Notes

The authors declare no competing financial interest.

ACKNOWLEDGMENT

The authors express their gratitude to Katja Hauer and Michael Galant for SPR measurements. Andreas Gollner is thanked for scientific discussions and proof-reading. Julian Fuchs, Andreas Bergner and Xiao-Ling Cockcroft are gratefully thanked for quantum-mechanical calculations. Susanne Mayer and Gabriele Glendinning are thanked for compound logistics. Helmut Bergner is thanked for ICP/MS measurements. Furthermore we the authors express their deep gratitude to Nathalie Harrer, Herwig Machat, Andreas Schrenk, Bernd Wellenzohn, Gorana Sijan and Ida Dinold.

ABBREVIATIONS

AA, amino acid; BM, biomarker; 2-HG, 2-hydroxyglutarate; LRE, long range electrostatics; NAD+/H, nicotinamide adenine dinucleotide; NOE, nuclear Overhauser effect; PHGDH, phosphoglycerate dehydrogenase; PSAT, phosphoserine

transaminase; PSPH, phosphoserine hydrolase; SBDD, structure based drug design; SSP, serine synthesis pathway; STD-NMR, Saturation Transfer Difference NMR; TCAC, tricarboxylic acid cycle; TNBC, triple negative breast cancer;

DEDICATION

This work is dedicated to Wolfgang Sommergruber on the occasion of his retirement.

ASSOCIATED CONTENT

Supporting Information. The Supporting Information is available free of charge on the ACS Publications website. This material is available free of charge via the Internet at http://pubs.acs.org.

- Biochemical Assays (HTS PHGDH inhibitor assay, diaphorase NADH counterscreen, 3-phosphoglycerate dehydrogenase (PHGDH) fluorescence intensity assay)
- Cellular Assays (^{13}C serine assay in MDA-MB-468 cells, cellular uptake assay)
- (Bio)Physical Methods (ICP-MS, surface plasmon resonance)

- NMR (high resolution mass spectroscopy)
- Protein (expression, chemoproteomics, protein crystallization
- Safety (CEREP Panel)
- Chromatography
- Synthetic Procedures
- HPLC traces of selected compounds
- Molecular formula strings (CSV)

In addition, all crystallographic data can be downloaded from https://www.rcsb.org/.

Authors will release the atomic coordinates and experimental data upon article publication.

PDB codes:

Compound 9	**6RIH**
Compound 15	**6RJ3**
Compound 39	**6RJ5**

Compound 40	6RJ2
BI-4924	6RJ6
3-PG	6CWA

REFERENCES

1. Hanahan, D.; Weinberg, Robert A. Hallmarks of Cancer: The Next Generation. *Cell* **2011,** 144, 646-674.

2. Zogg, C. K. Phosphoglycerate Dehydrogenase: Potential Therapeutic Target and Putative Metabolic Oncogene. *Journal of Oncology* **2014,** 2014, 524101.

3. Possemato, R.; Marks, K. M.; Shaul, Y. D.; Pacold, M. E.; Kim, D.; Birsoy, K.; Sethumadhavan, S.; Woo, H.-K.; Jang, H. G.; Jha, A. K.; Chen, W. W.; Barrett, F. G.; Stransky, N.; Tsun, Z.-Y.; Cowley, G. S.; Barretina, J.; Kalaany, N. Y.; Hsu, P. P.; Ottina, K.; Chan, A. M.; Yuan, B.; Garraway, L. A.; Root, D. E.; Mino-Kenudson, M.; Brachtel, E. F.; Driggers, E. M.; Sabatini, D. M. Functional Genomics Reveal that the Serine Synthesis Pathway is Essential in Breast Cancer. *Nature* **2011,** 476, 346.

4. Locasale, J. W.; Grassian, A. R.; Melman, T.; Lyssiotis, C. A.; Mattaini, K. R.; Bass, A. J.; Heffron, G.; Metallo, C. M.; Muranen, T.; Sharfi, H.; Sasaki, A. T.; Anastasiou, D.; Mullarky, E.; Vokes, N. I.; Sasaki, M.; Beroukhim, R.; Stephanopoulos,

G.; Ligon, A. H.; Meyerson, M.; Richardson, A. L.; Chin, L.; Wagner, G.; Asara, J. M.; Brugge, J. S.; Cantley, L. C.; Vander Heiden, M. G. Phosphoglycerate Dehydrogenase Diverts Ggycolytic Flux and Contributes to Oncogenesis. *Nature Genetics* **2011,** 43, 869.

5. Mullarky, E.; Mattaini, K. R.; Vander Heiden, M. G.; Cantley, L. C.; Locasale, J. W. PHGDH Amplification and Altered Glucose Metabolism in Human Melanoma: PHGDH Amplification and Altered Glucose Metabolism. *Pigment Cell & Melanoma Research* **2011,** 24, 1112-1115.

6. Song, Z.; Feng, C.; Lu, Y.; Lin, Y.; Dong, C. PHGDH is an Independent Prognosis Marker and Contributes Cell Proliferation, Migration and Invasion in Human Pancreatic Cancer. *Gene* **2018,** 642, 43-50.

7. Yoshino, H.; Nohata, N.; Miyamoto, K.; Yonemori, M.; Sakaguchi, T.; Sugita, S.; Itesako, T.; Kofuji, S.; Nakagawa, M.; Dahiya, R.; Enokida, H. PHGDH as a Key Enzyme for Serine Biosynthesis in HIF2α-targeting Therapy for Renal Cell Carcinoma. *Cancer research* **2017,** 77, 6321-6329.

8. Fenner, A. PHGDH is Key for Targeting HIF in RCC. *Nature Reviews Urology* **2017,** 14, 702.

9. DeNicola, G. M.; Chen, P.-H.; Mullarky, E.; Sudderth, J. A.; Hu, Z.; Wu, D.; Tang, H.; Xie, Y.; Asara, J. M.; Huffman, K. E.; Wistuba, I. I.; Minna, J. D.; DeBerardinis, R. J.; Cantley, L. C. NRF2 Regulates Serine Biosynthesis in Non-small Cell Lung Cancer. *Nature genetics* **2015,** 47, 1475-1481.

10. Hamanaka, R. B.; Nigdelioglu, R.; Meliton, A. Y.; Tian, Y.; Witt, L. J.; O'Leary, E.; Sun, K. A.; Woods, P. S.; Wu, D.; Ansbro, B.; Ard, S.; Rohde, J. M.; Dulin, N. O.; Guzy, R. D.; Mutlu, G. M. Inhibition of Phosphoglycerate Dehydrogenase Attenuates Bleomycin-induced Pulmonary Fibrosis. *Am. J. Respir. Cell Mol. Biol.* **2017,** 58, 585-593.

11. Zhang, B.; Zheng, A.; Hydbring, P.; Ambroise, G.; Ouchida, A. T.; Goiny, M.; Vakifahmetoglu-Norberg, H.; Norberg, E. PHGDH Defines a Metabolic Subtype in Lung Adenocarcinomas with Poor Prognosis. *Cell Reports* **2017,** 19, 2289-2303.

12. Noh, S.; Kim, D. H.; Jung, W. H.; Koo, J. S. Expression Levels of Serine/Glycine Metabolism-related Proteins in Triple Negative Breast Cancer Tissues. *Tumor Biology* **2014,** 35, 4457-4468.

13. Jia, X.-Q.; Zhang, S.; Zhu, H.-J.; Wang, W.; Zhu, J.-H.; Wang, X.-D.; Qiang, J.-F. Increased Expression of PHGDH and Prognostic Significance in Colorectal Cancer. *Transl Oncol* **2016,** 9, 191-196.

14. Zheng, M.; Guo, J.; Xu, J.; Yang, K.; Tang, R.; Gu, X.; Li, H.; Chen, L. Ixocarpalactone A from Dietary Tomatillo Inhibits Pancreatic Cancer Growth by Targeting PHGDH. *Food & Function* **2019**.

15. Locasale, J. W. Serine, Glycine and the One-Carbon Cycle: Cancer Metabolism in Full Circle. *Nature reviews. Cancer* **2013,** 13, 572-583.

16. Mattaini, K. R.; Sullivan, M. R.; Vander Heiden, M. G. The Importance of Serine Metabolism in Cancer. *The Journal of Cell Biology* **2016,** 214, 249-257.

17. Tedeschi, P. M.; Markert, E. K.; Gounder, M.; Lin, H.; Dvorzhinski, D.; Dolfi, S. C.; Chan, L. L. Y.; Qiu, J.; DiPaola, R. S.; Hirshfield, K. M.; Boros, L. G.; Bertino, J. R.; Oltvai, Z. N.; Vazquez, A. Contribution of Serine, Folate and Glycine Metabolism to the ATP, NADPH and Purine Requirements of Cancer Cells. *Cell Death & Disease* **2013,** 4, e877.

18. Reid, M. A.; Allen, A. E.; Liu, S.; Liberti, M. V.; Liu, P.; Liu, X.; Dai, Z.; Gao, X.; Wang, Q.; Liu, Y.; Lai, L.; Locasale, J. W. Serine Synthesis Through PHGDH Coordinates Nucleotide Levels by Maintaining Central Carbon Metabolism. *Nature Communications* **2018,** 9, 5442.

19. Zhang, X.; Bai, W. Repression of Phosphoglycerate Dehydrogenase Sensitizes Triple-negative Breast Cancer to Doxorubicin. *Cancer Chemotherapy and Pharmacology* **2016,** 78, 655-659.

20. Fan, J.; Teng, X.; Liu, L.; Mattaini, K. R.; Looper, R. E.; Vander Heiden, M. G.; Rabinowitz, J. D. Human Phosphoglycerate Dehydrogenase Produces the Oncometabolite d-2-Hydroxyglutarate. *ACS Chemical Biology* **2015,** 10, 510-516.

21. Figueroa, M. E.; Abdel-Wahab, O.; Lu, C.; Ward, P. S.; Patel, J.; Shih, A.; Li, Y.; Bhagwat, N.; Vasanthakumar, A.; Fernandez, H. F.; Tallman, M. S.; Sun, Z.; Wolniak, K.; Peeters, J. K.; Liu, W.; Choe, S. E.; Fantin, V. R.; Paietta, E.; Löwenberg, B.; Licht, J. D.; Godley, L. A.; Delwel, R.; Valk, P. J. M.; Thompson, C. B.; Levine, R. L.; Melnick, A. Leukemic IDH1 and IDH2 Mutations Result in a Hypermethylation Phenotype,

Disrupt TET2 Function, and Impair Hematopoietic Differentiation. *Cancer cell* **2010,** 18, 553-567.

22. Borodovsky, A.; Seltzer, M. J.; Riggins, G. J. Altered Cancer Cell Metabolism in Gliomas with Mutant IDH1 or IDH2. *Current Opinion in Oncology* **2012,** 24, 83-89.

23. Yoshino, J.; Imai, S.-i. Accurate Measurement of Nicotinamide Adenine Dinucleotide (NAD(+)) with High-Performance Liquid Chromatography. *Methods in molecular biology (Clifton, N.J.)* **2013,** 1077, 203-215.

24. Chen, J.; Chung, F.; Yang, G.; Pu, M.; Gao, H.; Jiang, W.; Yin, H.; Capka, V.; Kasibhatla, S.; Laffitte, B.; Jaeger, S.; Pagliarini, R.; Chen, Y.; Zhou, W. Phosphoglycerate Dehydrogenase is Dispensable for Breast Tumor Maintenance and Growth. *Oncotarget* **2013,** 4, 2502-2511.

25. Mullarky, E.; Lucki, N. C.; Beheshti Zavareh, R.; Anglin, J. L.; Gomes, A. P.; Nicolay, B. N.; Wong, J. C. Y.; Christen, S.; Takahashi, H.; Singh, P. K.; Blenis, J.; Warren, J. D.; Fendt, S.-M.; Asara, J. M.; DeNicola, G. M.; Lyssiotis, C. A.; Lairson, L. L.; Cantley, L. C. Identification of a Small Molecule Inhibitor of 3-Phosphoglycerate Dehydrogenase to Target Serine Biosynthesis in Cancers. *Proceedings of the National Academy of Sciences* **2016,** 113, 1778-1783.

26. Pacold, M. E.; Brimacombe, K. R.; Chan, S. H.; Rohde, J. M.; Lewis, C. A.; Swier, L. J. Y. M.; Possemato, R.; Chen, W. W.; Sullivan, L. B.; Fiske, B. P.; Cho, S. W.; Freinkman, E.; Birsoy, K.; Abu-Remaileh, M.; Shaul, Y. D.; Liu, C. M.; Zhou, M.; Koh, M. J.; Chung, H.; Davidson, S. M.; Luengo, A.; Wang, A. Q.; Xu, X.; Yasgar, A.; Liu, L.; Rai,

G.; Westover, K. D.; Vander Heiden, M. G.; Shen, M.; Gray, N. S.; Boxer, M. B.; Sabatini, D. M. A PHGDH Inhibitor Reveals Coordination of Serine Synthesis and 1-Carbon Unit Fate. *Nature chemical biology* **2016,** 12, 452-458.

27. Ravez, S.; Corbet, C.; Spillier, Q.; Dutu, A.; Robin, A. D.; Mullarky, E.; Cantley, L. C.; Feron, O.; Frédérick, R. α-Ketothioamide Derivatives: A Promising Tool to Interrogate Phosphoglycerate Dehydrogenase (PHGDH). *J. Med. Chem.* **2017,** 60, 1591-1597.

28. Wang, Q.; Liberti, M. V.; Liu, P.; Deng, X.; Liu, Y.; Locasale, J. W.; Lai, L. Rational Design of Selective Allosteric Inhibitors of PHGDH and Serine Synthesis with Anti-tumor Activity. *Cell Chemical Biology* **2017,** 24, 55-65.

29. Fuller, N.; Spadola, L.; Cowen, S.; Patel, J.; Schönherr, H.; Cao, Q.; McKenzie, A.; Edfeldt, F.; Rabow, A.; Goodnow, R. An Improved Model for Fragment-based Lead Generation at AstraZeneca. *Drug Discovery Today* **2016,** 21, 1272-1283.

30. Unterlass, J. E.; Basle, A.; Blackburn, T. J.; Tucker, J.; Cano, C.; Noble, M. E. M.; Curtin, N. J. Validating and Enabling Phosphoglycerate Dehydrogenase (PHGDH) as a Target for Fragment-based Drug Discovery in PHGDH-amplified Breast Cancer. *Oncotarget* **2018,** 9, 13139-13153.

31. Raze Therapeutics, I.; Mainolfi, N.; Moyer, M. P. 3-Phosphoglycerate dehydrogenase Inhibitors and uses thereof. WO2017156177, 2017.

32. Rohde, J. M.; Brimacombe, K. R.; Liu, L.; Pacold, M. E.; Yasgar, A.; Cheff, D. M.; Lee, T. D.; Rai, G.; Baljinnyam, B.; Li, Z.; Simeonov, A.; Hall, M. D.; Shen, M.; Sabatini,

D. M.; Boxer, M. B. Discovery and Optimization of Piperazine-1-Thiourea-based Human Phosphoglycerate Dehydrogenase Inhibitors. *Biorg. Med. Chem.* **2018,** 26, 1727-1739.

33. Baell, J. B.; Holloway, G. A. New Substructure Filters for Removal of Pan Assay Interference Compounds (PAINS) from Screening Libraries and for Their Exclusion in Bioassays. *J. Med. Chem.* **2010,** 53, 2719-2740.

34. Ward, R. A.; Brassington, C.; Breeze, A. L.; Caputo, A.; Critchlow, S.; Davies, G.; Goodwin, L.; Hassall, G.; Greenwood, R.; Holdgate, G. A.; Mrosek, M.; Norman, R. A.; Pearson, S.; Tart, J.; Tucker, J. A.; Vogtherr, M.; Whittaker, D.; Wingfield, J.; Winter, J.; Hudson, K. Design and Synthesis of Novel Lactate Dehydrogenase A Inhibitors by Fragment-Based Lead Generation. *J. Med. Chem.* **2012,** 55, 3285-3306.

35. Mayer, M.; Meyer, B. Characterization of Ligand Binding by Saturation Transfer Difference NMR Spectroscopy. *Angew. Chem. Int. Ed.* **1999,** 38, 1784-1788.

36. Unterlass, J. E.; Wood, R. J.; Basle, A.; Tucker, J.; Cano, C.; Noble, M. M. E.; Curtin, N. J. Structural Insights into the Enzymatic Activity and Potential Substrate Promiscuity of Human 3-Phosphoglycerate Dehydrogenase (PHGDH). *Oncotarget* **2017,** 8, 104478-104491.

37. Hoffmann, R. W. Allylic 1,3-Strain as a Controlling Factor in Stereoselective Transformations. *Chem. Rev.* **1989,** 89, 1841-1860.

38. Tietze Lutz, F.; Schulz, G. Ab Initio Molecular Orbital Calculations on Allylic 1,3-Strain of Electron-Donor- and Electron-Acceptor-Substituted Alkenes. *Liebigs Annalen* **1996,** 1996, 1575-1579.

39. Ravez, S.; Spillier, Q.; Marteau, R.; Feron, O.; Frédérick, R. Challenges and Opportunities in the Development of Serine Synthetic Pathway Inhibitors for Cancer Therapy. *J. Med. Chem.* **2017,** 60, 1227-1237.

40. Caravella, J. A.; Carbeck, J. D.; Duffy, D. C.; Whitesides, G. M.; Tidor, B. Long-Range Electrostatic Contributions to Protein−Ligand Binding Estimated Using Protein Charge Ladders, Affinity Capillary Electrophoresis, and Continuum Electrostatic Theory. *J. Am. Chem. Soc.* **1999,** 121, 4340-4347.

41. Vallet, V.; Wahlgren, U.; Grenthe, I. Chelate Effect and Thermodynamics of Metal Complex Formation in Solution: A Quantum Chemical Study. *J. Am. Chem. Soc.* **2003,** 125, 14941-14950.

42. Vonrhein, C.; Flensburg, C.; Keller, P.; Sharff, A.; Smart, O.; Paciorek, W.; Womack, T.; Bricogne, G. Data Processing and Analysis with the autoPROC toolbox. *Acta Crystallogr D Biol Crystallogr* **2011,** 67, 293-302.

43. Collaborative Computational Project, N. The CCP4 Suite: Programs for Protein Crystallography. *Acta Crystallographica Section D* **1994,** 50, 760-763.

44. Emsley, P.; Lohkamp, B.; Scott, W. G.; Cowtan, K. Features and Development of Coot. *Acta Crystallographica Section D* **2010,** 66, 486-501.

45. Bricogne, G.; Blanc, E.; Brandl, M.; Flensburg, C.; Keller, P.; Paciorek, W.; Roversi, P.; Sharff, A.; Smart, O.; Vonrhein, C.; Womack, T. BUSTER version 2.11.5. **2011**.

TABLE OF CONTENTS GRAPHIC

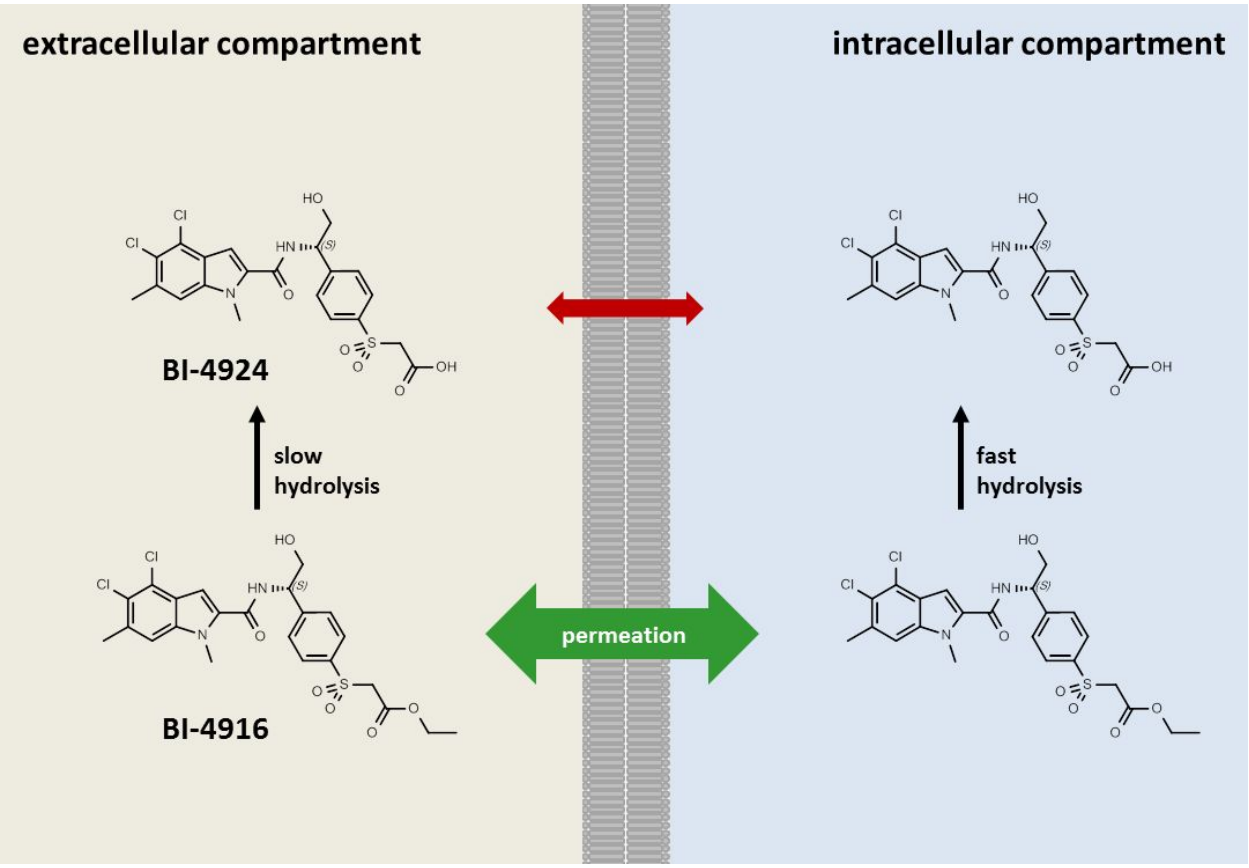

End of Document